# Notes for PHYS 234: High Energy Astrophysics

Bill Wolf

May 20, 2013

# Contents

# 1 Introduction

*Monday, April 1, 2013*

## 1.1 What is High Energy Astrophysics?

There are many definitions, but one is that high energy astrophysics is "the study of the violent and extreme processes in the universe." Another traditional definition is the study of processes that produce gamma rays and X-rays (possibly ultraviolet radiation as well). Unfortunately, such high energy photons are very effectively blocked by the Earth's atmosphere, so observations are limited to being taken from the upper atmosphere or space. As a result, high energy astrophysics is a relatively young subfield of astrophysics ($\lesssim 100$ yrs).

For our purposes, we will take an expanded view of what high energy astrophysics is, including white dwarfs (WDs), supernovae (SNe), and other phenomena.

## 1.2 How is the High Energy Sky Different?

In this course, we will deal with energy in terms of electron volts (eV). A common photon energy of interest to us has an energy of 1 MeV, which is roughly equivalent to 1 million optical photons (which are thus obviously about 1 eV in energy). If we fix energy, high energy (HE) events must produce fewer photons since each is carrying more energy. In addition to smaller photon counts, HE events are rarer, so there are far fewer sources in the sky at any given moment. There are on the order of $10^5$ bright X-Ray sources (detectable by Chandra), on the order of $10^3$ bright gamma ray objects (detectable by Fermi), about 50 events that are bright around 100 MeV, and dozens of objects with energies of TeVs. Additionally, we observe catastrophic fast and transient events that are here and gone again.

## 1.3 High Energy Photons

Traditionally 0.1 keV $-$ 100 TeV constitute "high energy photons". Some basic units are presented in Table 1. Related to those, a few other relations of interest are presented in Table 2. As we'll see, the messengers of HE processes are all over the EM spectrum, particularly at radio wavebands. Additionally, neutrinos, particles, and gravity waves get in the mix, giving rise to the phrase "multi-messenger" astrophysics.

| Symbol | Value | Units |
|---|---|---|
| $h$ | $6.626 \times 10^{-27}$ | erg s |
| 1 eV | $1.602 \times 10^{-12}$ | erg |
| 1 Å | $10^{-8}$ | cm |
| $r_{\rm proton}$ | $\sim 10^{-13}$ | cm |

Table 1: Essential units in HE Astrophysics

## 1.4 History

R ontgen discovered X-rays in 1895, earning him the Nobel prize in 1901. In 1914, Henry Moseley developed the use of spectroscopy for HE processes through Moseley's Law in 1914. A bit earlier, Victor Hess discovered cosmic rays (1912) through the use of balloon experiments. He found that there was more ionization farther from Earth, indicating a new as of yet undiscovered source of ionizing radiation, earning him the Nobel Prize in 1936. In 1962, Giacconi used sounding rockets to contribute significantly to the study of X-rays. In particular, he discovered Sco X-I. His efforts in X-Ray astronomy earned him the Nobel prize in 2002.

In 1977, the first X-ray satellite went into orbit, HEAO-I, which had a bandwidth of 0.2 keV - 10 MeV. It detected 842 discrete sources. Later HEAO-2 (later renamed Einstein) was launched with a bandwidth of 0.1 keV - 20 keV. This was the first X-ray telescope capable of focussing incoming radiation. In 1992, the Compton Gamma Ray Observatory (CRGO) was launched. It allowed gamma ray bursts to be localized. Previously, gamma ray bursts were of unknown origins. In 1999, Chandra was launched, which is also able to focus X-Rays. More recently, Fermi was launched in 2008, which is a gamma ray focusing telescope. Of particular interest is the LAT (Large Area Telescope) which allows detections of extremely high energy photons. To date, the newest satellite is NuStar, which was launched in 2012 and excels in spectroscopy of high energy sources.

## 1.5 X-Ray Spectra and Moseley's Law

The *continuum* in X-Ray sources is caused by Bremsstrahlung "braking radiation" (free-free). Essentially an electron scatters off a proton and emits an X-ray in the process. The *lines* in the spectra are **K-shell** emissions. This is similar to H$\alpha$ emission, but on heavier elements. Essentially, an electron from a low shell is ejected, allowing a higher $n$ electron to fall to the ground ($K$) shell, emitting in the X-ray.

Moseley's Law states that the shell energy scales like the atomic number to the second power. It is then analogous to the Bohr atom (K$\alpha \sim$ H$\alpha$). Transition energies are then given by

$$h\nu = 13.6\,\mathrm{eV}(Z-1)^2 \left[\frac{1}{n_f^2} - \frac{1}{n_i}^2\right] \tag{1.1}$$

$$= 13.6\,\mathrm{eV}(Z-1)^2 \left[\frac{1}{1} - \frac{1}{2^2}\right] \tag{1.2}$$

Equation (1.2) is the K$\alpha$ line for a ion with atomic number $Z$ with an $n = 1$ electron kicked out ahead of time. This law accurately reflects the energies of lines we observe in X-Ray spectra.

| Symbol | Value | Units |
|---|---|---|
| 1 erg | 624 | GeV |
| $m_e c^2$ | 511 | keV |
| $m_p c^2$ | 931 | MeV |
| 1 keV / $k$ | $11.6 \times 10^6$ | K |
| 1 keV / $c$ | $242 \times 10^{17}$ Hz | |

Table 2: Additional energy scales

## 1.6 Detectors

There are three main ways to stop HE photons

1. Photoelectric absorption:
$$\gamma + \text{atom} \to \text{atom}^+ + e^-$$

2. Compton Scattering:
$$\gamma + e^- \to \gamma + e^-$$
This is essentially the high energy limit of Thomson scattering which allows for energy transfer

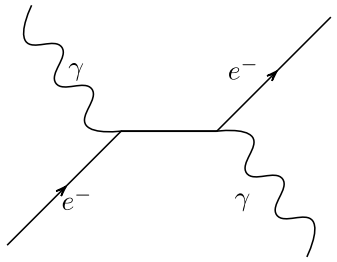


Figure 1: Schematic of Compton Scattering

3. Pair Production
$$\gamma + \text{nucleus} \to e^+ + e^- + \text{nucleus}$$
The nucleus is required to appease conservation laws

All three of these have been used to make HE photon detectors since they can generate measurable electrons. To characterize the absorption of photons in a material through some characteristic wavelength $\ell$, we'll assume there is some initial intensity $I$ of HE photons. This intensity if attenuated according to
$$I = I_0 e^{-\left(\frac{\mu}{\rho}\right)\rho\ell} \tag{1.3}$$
where $\rho$ is the density of the material and $\mu/\rho$ is the "mass attenuation" (similar to an opacity), given by
$$\frac{\mu}{\rho} = \underbrace{\frac{\sigma}{\rho}}_{\text{Compton}} + \underbrace{\frac{\tau}{\rho}}_{\text{photoelectric}} + \underbrace{\frac{\kappa}{\rho}}_{\text{pair production}} \tag{1.4}$$
Knowing how your detector material is sensitive to each of the HE photon stoppage sources is essential to designing an effective HE photon telescope. Now we'll discuss some different types of HE detectors.

*Wednesday, April 3, 2013*

**Gas Proportional Counters** A gas of Argon and (other stuff?) absorbs HE photons, which then give off free electrons which are collected and counted. This is essentially Geiger counter. Each interaction causes multiple ionizations, so we are able to detect individual photons.

**Scintillation Counters** This detector relies on a crystal with doping, providing so-called "actuator sites". Incoming photons create an electron-hole pair which gets re-radiated at the actuator site around 4200Å. This process is about 12% efficient. The produced light then interacts with a photomultiplier tube.

**Solid State** Solid State detectors function much like CCDs from optical astronomy, but using materials that are better suited to HE photons.

These detectors will count HE photons, but they do not provide directional information, like a camera with no telescope. So now we'll talk about different telescopes used for HE astrophysics. One big problem in such telescopes is that focussing is very difficult. In deed, HE photons will pass through mirrors unless glancing at an angle of three degrees or less. In 1952, Wolter came up with a way to effective focus X-rays using a barrel of parabolic and hyperbolic mirrors to gradually focus the X-rays through a series of many gentle reflections. As an example, NuStar will use 130 concentric mirrors to focus X-rays with energies as high as 79 keV. Chandra, XMM, HEAO-2/Einstein all work in this manner. Parabolic mirrors would focus an image onto a point, so hyperboloids are employed to focus images onto a plane, giving a field of view.

At higher energies, HE astronomers use **coded aperture masks**. These devices have a pattern of transparent and opaque partitions which will project different observed patterns at different angles. These differing patterns can be analyzed to reproduce an image. This technology is used by HETE-2, Swift, and Integral.

Additionally, we use Compton scattering and pair production devices to detect very high energy photons. Here, a gamma ray can interact with a Tungsten foil, causing pair production, which can be detected via a calorimeter. This is how the LAT instrument on Fermi works.

| Energy | $T_{\text{thermal}}$ | Process |
|---|---|---|
| $< 10\,\text{keV}$ | $< 10^8$ K | $K$ and $L$ shell line emission, Bremsstrahlung, thermal blackbody |
| $10\,\text{keV} - 10\,\text{MeV}$ | - | non-thermal processes: isomeric transitions from metastable isomers (gamma ray lines), e.g. $^{60}\text{Co} \rightarrow {}^{60}\text{Ni} + e^- + \bar{\nu}_e + 1.15\,\text{MeV}$ (present in supernova remnants) |
| $511\,\text{keV}$ | $10^9$ K | $m_e c^2$ annihilation lines (seen in galactic center). E.g. $e^- + e^+ \rightarrow \gamma + \gamma$ |
| 140 MeV − 10 GeV | $10^{12}$ K | Pion decay (strong force) |
| $> 10$ GeV | - | non-thermal processes: inverse Compton scattering, shock acceleration |

Table 3: Different sources of high energy photons.

At the very highest energies, we must go back to the ground in order to use air showers. Such instruments include HESS, CANGAROO, and VRITAS. Here, a cosmic ray interacts with the air, moving faster than the local speed of light. This in tern, causes a cone of Cerenkov radiation. With an array of detectors, the air shower can be detected and the angle of the cone can be ascertained, giving the energy of the cosmic ray. Typically we get 100 optical photons per square meter for each 100 GeV photon.

Note that, beyond photons, HE processes produce other objects of interest. **Cosmic rays** are essentially high energy protons, electrons, nuclei, and other charged particles. Low energy neutrinos are produced through inverse beta decays ($p+e^- \rightarrow n+\nu_e$). High energy neutrinos come from... pion stuff ($\gamma + p \rightarrow n + \pi^+$, $\pi^+ \rightarrow \mu + \nu_\mu$). Finally, we can observe (ostensibly) gravity waves from rapidly changing gravitational fields.

## 1.7 Radioactivity

In 1898, Henri Becquerel discovered radioactivity by examining how uranium salts interacted with photographic plates. The actual term "radioactive" was coined by Marie and Pierre Curie. It was Rutherford in 1899 who first came up with the nomenclature of $\alpha$, $\beta$, and $\gamma$ rays, which are ordered in increasing penetration capability. Now we know that they are completely different things: helium nuclei, electrons, and... well... $\gamma$-rays.

## 1.8 Energetics

In stellar evolution, we learn that gravitational energy is not a primary source of energy except in early formation and late collapse phases. Even in the core collapse scenario, most of the gravitational energy is lost in the form of neutrinos. In general, then, gravitational binding energy release is unimportant to most stars most of the time. Other scales of energy release can be important though.

Chemical reactions give only a few eV per baryon. For instance 10 eV per baryon corresponds to $10^{13}$ erg/g. Chemical processes are not really important in astronomy as energy sources.

Nucleosynthesis, on the other hand, gives about 1 MeV per baryon, equivalent to $10^{18}$ erg/g. Note that the greatest gains in nucleosynthesis come from the simplest steps (like hydrogen to helium). Higher burning gives less and less energy, and eventually at Iron, there are no more energy gains to be had.

Accretion power is more efficient still since it scales as $GM/R$. For the sun, this corresponds to about $2 \times 10^{15}$ erg/g. One proposed explanation for the energy source for the sun was gravitational contraction. If we take the gravitational energy of the sun and divide by its current luminosity, we get a lifetime on the order of $10^7$ years– far too short to account for how long it has been shining on Earth. Quasi-stellar objects (QSOs), on the other hand, are powered by the accretion of matter (not nuclear powered!). We observe them at $L_{\rm QSO} \sim 10^{47}$ erg/s. If this was powered by nuclear reactions, there would need to be about $10^{12}$ $M_\odot$ of matter burned each Gyr to provide the power! Mass estimates for these objects are only as high as $10^{11}$, so they are likely powered by accretion.

# 2 Accretion of Astrophysical Plasmas

## 2.1 Spherical Flow onto Compact Objects

Now we will consider the spherically symmetric accretion of matter onto a compact object. This essentially ignores angular momentum, which will be included at a later time when we discuss accretion disks.

There is a fundamental limit on the rate at which matter can be accreted, called the **Eddington Limit**.

*Monday, April 8, 2013*

This limiting accretion rate is achieved when outward radiation pressure is perfectly balanced with inward gravity. Consider a fully-ionized medium of pure hydrogen (protons and electrons) The gravitational force for a given particle is

$$F_{\rm grav} \approx -\frac{GM(m_{\rm particle})}{r^2} \sim -\frac{GMm_p}{r^2} \tag{2.1}$$

Now we'll define a number flux of photons at a particular frequency via

$$S_\nu = \frac{L_{\rm Edd}}{4\pi r^2 h\nu} \tag{2.2}$$

We'll assume that radiative transfer is dominated by Thomson scattering, which gives an effective cross section of

$$\sigma_{\rm T} = \sum_i \frac{2}{3}\left(\frac{e_i^2}{m_i c^2}\right)^2 \tag{2.3}$$

Since the proton is $\sim 2000$ times more massive than an electron, the electron dominates the cross section. With this in hand, we want to find the force due to radiation pressure,

$$F_{\rm rad} = \sigma_{\rm T} S_\nu p = \frac{\sigma_{\rm T} L}{4\pi r^2 c} \tag{2.4}$$

where $p$ is the momentum of a photon with frequency $\nu$, namely $p = h\nu/c$. We can now solve for the Eddington Luminosity:

$$L_{\rm Edd} = \frac{4\pi G m_p c M}{\sigma_{\rm T}} \tag{2.5}$$

where we've set $F_{\rm grav}$ equal to $F_{\rm rad}$. Parameterizing to solar masses, this gives a luminosity of

$$L_{\rm Edd} = 1.3\times 10^{38}\left(\frac{M}{M_\odot}\right)\ {\rm erg\ s^{-1}} = 6.5\times 10^4\left(\frac{M}{M_\odot}\right) L_\odot \tag{2.6}$$

This it the fundamental luminosity of a star or accreting object. Luminosities higher than this would result in mass loss. If an object shining at the Eddington luminosity radiates as a blackbody, we can find a characteristic temperature (at a given radius and mass):

$$T_{\rm eff} = \left(\frac{cGMm_p}{R^2\sigma_{\rm T}\sigma_{\rm B}}\right)^{1/4} \tag{2.7}$$

For a neutron star, this corresponds to $kT \approx 1.9$ keV and for a white dwarf, $kT \approx 53$ eV. This is essentially the shock energy of infalling particles of accreted matter.

There is an effective accretion rate, $\dot{M}$ that corresponds to $L_{\rm Edd}$ if we assume that all of the luminosity is liberated at the edge of the star. The accretion luminosity is given by

$$L_{\rm acc} \approx \frac{GM\dot{M}}{R} \tag{2.8}$$

Equating this to the Eddington luminosity gives us the limiting accretion rate:

$$\dot{M}_{\rm Edd} = \frac{4\pi m_p c R}{\sigma_{\rm T}} \tag{2.9}$$

For a neutron star, this corresponds to $\dot{M} \sim 10^{-8}\, M_\odot/{\rm yr}$ and for a white dwarf, $\dot{M} \sim 10^{-5}\, M_\odot/{\rm yr}$. The accretion rate indicated by the capture rate of plasma by a central object must depend on properties at large distances as well as the mass of the central object. All other dynamics should be dictated by the background material as well as the pull of the large central mass.

We then define $\rho(\infty)$ to be the density at a sufficiently large distance away from the central object. Similarly, $c_s(\infty)$ and $T(\infty)$ are the asymptotic sound speed and temperature, respectively. We'll assume material at this sufficiently far enough distance starts at rest with respect to the bulk plasma. The capture rate can be modeled to be

$$\dot{M} = \pi r_{\rm cap}^2 v_{\rm eff} \rho(\infty) \tag{2.10}$$

where $r_{\rm cap}$ designates the radius to which the central mass is able to influence the background medium and $v_{\rm eff}$ is the effective velocity at the capture radius. If the particles are streaming by the mass, $r_{\rm cap}$ must be related to some typical velocity (for instance, the velocity of a passing wind). If at rest, though, $r_{\rm cap}$ is related to the sound speed, $c_s$. In fact, we know that $c_s^2$ is just the thermal energy per unit mass (up to a factor of two), so we may specify

$$c_s(\infty) \sim \sqrt{\frac{kT}{m_{\rm H}}} \sim 10\,{\rm km/s}\sqrt{\frac{T}{10^8\,{\rm K}}} \tag{2.11}$$

Setting the asymptotic sound speed equal to the escape velocity, $c_s \sim \sqrt{GM/r_{\rm cap}}$, we find the capture radius for static plasma to be

$$r_{\rm cap} = \frac{GM}{c_s^2(\infty)} \tag{2.12}$$

Now identifying $v_{\rm eff}$ and $c_s(\infty)$, we arrive at an accretion rate

$$\dot{M} \approx \frac{\pi G^2 M^2}{c_s^4(\infty)} c_s(\infty)\rho(\infty) = \frac{\pi G^2 M^2 \rho(\infty)}{c_s^3(\infty)} \tag{2.13}$$

To get some intuition, let's assume a number density of $n = 1$ cm$^{-3}$, which corresponds to $\rho = 1.6 \times 10^{-24}$ g/cm$^3$, and a sound speed of $c_s = 10^6\,{\rm cm/s}\sqrt{T/10^4\ {\rm K}}$. For a $1.4\,M_\odot$ neutron star, this give a capture rate of

$$\dot{M} = 1.8 \times 10^{11}\,{\rm g/s}\left(\frac{M}{1.4 M_\odot}\right)^2\left(\frac{n}{1\,{\rm cm^{-3}}}\right)\left(\frac{T}{10^4\,{\rm K}}\right)^{-3/2} \sim 10^{-15}\, M_\odot/{\rm yr} \tag{2.14}$$

## 2.2 A More Detailed Calculation

Any treatment of accretion of plasma must satisfy the continuity equation (essentially mandating mass conservation), namely

$$\frac{\partial \rho}{\partial t} + \boldsymbol{\nabla} \cdot (\rho \mathbf{v}) = 0 \tag{2.15}$$

In a steady state, the time derivative must vanish, leaving us with simply

$$\boldsymbol{\nabla} \cdot (\rho \mathbf{v}) = 0 \tag{2.16}$$

$\rho\mathbf{v}$ is essentially the mass flux. Its divergence is the net flux of mass per unit volume (a positive value would mean mass is accumulating at point and a negative value would mean that mass is being depleted from a point). We will assume spherically symmetric inflow ($\mathbf{v} = -v\,\hat{r}$). The continuity equation then tells us

$$\frac{1}{r^2}\frac{d}{dr}\left(r^2 \rho v\right) = 0 \qquad \Rightarrow \qquad r^2 \rho v = \text{constant} \tag{2.17}$$

We can also write down an accretion rate given the mass flux:

$$\dot{M} = 4\pi r^2 \rho v \tag{2.18}$$

which allows us to eliminate the velocity via

$$v = \frac{\dot{M}}{4\pi r^2 \rho} \tag{2.19}$$

In addition to conserving mass, we must conserve momentum, introducing the Euler equation:

$$-\boldsymbol{\nabla} P + \mathbf{f} = \rho \frac{\partial \mathbf{v}}{dt} + (\rho \mathbf{v} \cdot \boldsymbol{\nabla})\mathbf{v} \tag{2.20}$$

where $\mathbf{f}$ is the external force density. Starting with the left side, we expand to get

$$-\boldsymbol{\nabla} P + \mathbf{f} = -\boldsymbol{\nabla} P - \frac{GM}{r^2}\rho\,\hat{r} \tag{2.21}$$

Now the right side of (2.20) is

$$\rho \frac{d\mathbf{v}}{dt} + \rho(\mathbf{v} \cdot \boldsymbol{\nabla})\mathbf{v} = -\boldsymbol{\nabla} P - \frac{GM}{r^2}\rho\,\hat{r} \tag{2.22}$$

Setting time derivatives to zero and simplifying, we get what we will refer to as our "Euler Equation":

$$\boxed{v\frac{dv}{dr} + \frac{1}{r}\frac{\partial P}{\partial r} + \frac{GM}{r^2} = 0} \tag{2.23}$$

*Wednesday, April 10, 2013*

We can assume a gas has a polytropic equation of state (eos) where pressure is related to density raised to a power following the form $\gamma = n/(n+1)$ for some (possibly infinite) $n$, called the **polytropic index**. Specifically, we assume

$$P = K\rho^{\gamma} = K\rho^{\frac{n}{n+1}} \tag{2.24}$$

As concrete examples, $\gamma = 5/3$ (or $n = 3/2$) is the index for an adiabatic, monatomic gas (yes, *that* gamma), and $\gamma = 1$ (or $n \to \infty$) is that for an isothermal ideal gas (reduction in the ideal gas law). The form of the ideal gas law that we'll use is

$$T = \frac{\mu m_H P}{\rho k} \tag{2.25}$$

where $\mu$ is the mean molecular weight, which is the mean mass per particle (electrons, nuclei, atoms, etc.) measure in amu, assuming $m_H \sim$ amu. Mathematically, we can write $\mu$ via

$$\mu = \frac{\rho}{n m_p} \tag{2.26}$$

So that for pure, ionized hydrogen we have $mu = 0.5$ (each atom splits into an electron and proton, so the mass for every two particles is $m_p$). For pure molecular hydrogen, $H_2$, then, we have $\mu = 2$.

We can rewrite hydrostatic equilibrium in terms of a sound speed, $c_s^2 = dP/dr$:

$$\frac{dP}{dr} = \frac{dP}{d\rho}\frac{d\rho}{dr} = c_s^2 \frac{d\rho}{dr} \tag{2.27}$$

Note that implicitly $c_s^2$ is a function of $r$. Now we rewrite eq. (2.23) as

$$v\frac{dv}{dr} + \frac{c_s^2}{\rho}\frac{d\rho}{dr} + \frac{GM}{r^2} = 0 \tag{2.28}$$

Now we'd like to get a handle on the term $\rho^{-1} d\rho/dr$. Recall that through the equation of continuity, $\partial_r(r^2 \rho v) = 0$. Expanding this result, we have

$$\rho \frac{\partial}{\partial r}(r^2 v) + r^2 v \frac{\partial \rho}{\partial r} = 0 \tag{2.29}$$

Dividing both sides by $\rho r^2 v$, we get the useful expression

$$\frac{1}{\rho}\frac{\partial \rho}{\partial v} = -\frac{1}{r^2 v}\frac{\partial}{\partial r}(r^2 v) \tag{2.30}$$

Substituting this into eq. (2.28) to get

$$\frac{1}{2}\frac{\partial}{\partial r}(v^2) + c_s^2\left(-\frac{1}{r^2 v}\frac{\partial}{\partial r}(r^2 v)\right) + \frac{GM}{r^2} = 0 \tag{2.31}$$

$$\frac{1}{2}\frac{\partial}{\partial r}(v^2) - \frac{c_s^2}{r^2 v}\left(2rv + r^2\frac{\partial v}{\partial r}\right) + \frac{GM}{r^2} = 0 \tag{2.32}$$

$$\frac{1}{2}\frac{\partial}{\partial r}v^2 - \frac{c_s^2}{v^2}\frac{1}{2}\frac{\partial}{\partial r}v^2 = -\frac{GM}{r^2} + \frac{2c_s^2}{r} \tag{2.33}$$

$$\frac{1}{2}\left(1 - \frac{c_s^2}{v^2}\right)\frac{\partial}{\partial r}v^2 = -\frac{GM}{r^2}\left(1 - \frac{2c_s^2 r}{GM}\right) \tag{2.34}$$

This final form is known as the **Parker Wind Equation** because Parker used it to describe the solar wind. In fact, this can be used to describe an outflowing wind as well as inflowing spherical

accretion.

Let's examine the near (small $r$) and far (large $r$) regimes in this equation. For the far case on the right hand side of eq. (2.34), we'll let $c_s \to c_s(\infty)$ at large distances (which also mandates that it be positive). On the left hand side, we would like $v(\infty) \to 0$. Or, as we move away, we want the velocity to steadily decrease, meaning $\partial_r(v^2) < 0$. At large $r$, we certainly know that the flow is subsonic ($v^2 < c_s^2$). So we define $r_s$ as the radius at which $1 - 2c_s^2 r/(GM) = 0$, or

$$\boxed{r_s = \frac{GM}{2c_s^2}} \tag{2.35}$$

Which is the so-called "sonic point". For $r < r_s$, the right hand side is negative, which then implies that $(1 - c_s^2/v^2)$ is *negative* and the flow is supersonic. Between these two regimes, the LHS must vanish, where $v_s^2 = c_s^2$ or $\partial_r v^2 = 0$ at the sonic point. Possible wind solutions are sketched in Figure 2. Now we'll return to the Euler equation and integrate it:

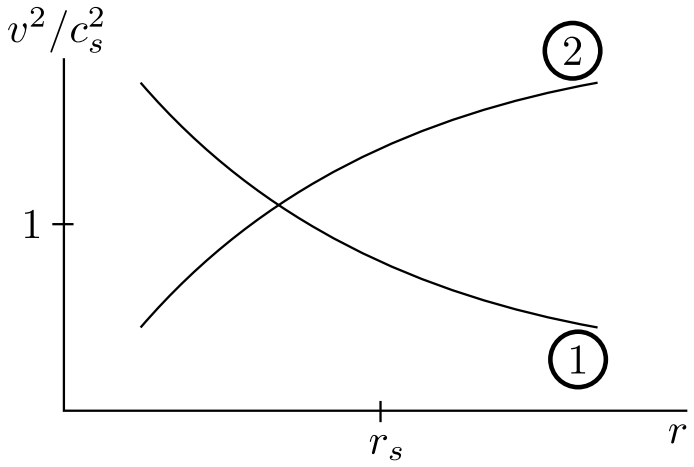


Figure 2: Possible wind solutions from the Parker wind equation. The curve labeled with a circled 1 is the case of accretion, where matter is subsonic past the sonic point and supersonic within. In this case, we expect freefall within the sonic point. The case marked with a circled 2 models a stellar wind, which is inverted.

$$\frac{v^2}{2} + \int \frac{dP}{\rho} - \frac{GM}{r} = \text{const} \tag{2.36}$$

Using our polytropic equation of state, we can express the pressure differential as

$$dP = K\gamma\rho^{\gamma-1}\, d\rho \qquad \Rightarrow \qquad c_s^2 = K\gamma\rho^{\gamma-1} = \frac{\gamma P}{\rho} \tag{2.37}$$

where we've utilized the definition of the sound speed to clean things up. Now eq. (2.36) becomes

$$\frac{v^2}{2} + \frac{c_s^2}{\gamma - 1} - \frac{GM}{\gamma} = \text{const} \tag{2.38}$$

This latest form is often referred to as the **Bernoulli integral**. Now we need to look at the boundary conditions. Specifically, we know that $v^2$ vanishes as $r \to \infty$, so the constant must be

$$\text{const} = \frac{[c_s(\infty)]^2}{\gamma - 1} \tag{2.39}$$

Additionally, we know that at $r = r_s$, $v = c_s$, so we may simplify to

$$c_s^2(r_s)\left[\frac{1}{2} + \frac{1}{\gamma - 1} - 2\right] = \frac{cs^2(\infty)}{\gamma - 1} \tag{2.40}$$

with this solution at hand, we can solve for the sound speed at the sonic point:

$$c_s(r_s) = c_s(\infty)\left(\frac{2}{5 - 3\gamma}\right)^{1/2} \tag{2.41}$$

Now we can return to our equation for the accretion rate in steady state:

$$\dot{M} = 4\pi r^2 \rho(-v) = 4\pi r_s^2 \rho(r_s) c_s(r_s) \tag{2.42}$$

Recall though that $c_s^2 \propto \rho^{\gamma-1}$. Then we also know $c_s^2(r_s)/c_s^2(\infty) = \rho(r_s)^{\gamma-1}/\rho(\infty)^{\gamma-1}$. Doing the algebra, this gives the density at the sonic point as

$$\rho(r_s) = \rho(\infty)\left[\frac{c_s(r_s)}{c_s(\infty)}\right]^{2/(\gamma-1)} \tag{2.43}$$

Doing all the substitutions, we get an accretion rate of

$$\boxed{\dot{M} = \pi G^2 M^2 \frac{\rho(\infty)}{c_s^3(\infty)}\left[\frac{2}{5 - 3\gamma}\right]^{\frac{5-3\gamma}{2(\gamma-1)}}} \tag{2.44}$$

This is the main result of Bondi accretion. Note that the term in the brackets is unity for $\gamma = 5/3$ and $e^{3/2} \approx 4.5$ for $\gamma = 1$. Bondi-Hoyle-Lyttleton accretion is where movement $v(\infty)$ of the body with respect to the gas is $\sqrt{c_s^2(\infty) + v^2(\infty)}$ which gives an accretion rate of

$$\dot{M} = 4\pi G^2 M^2 \frac{\rho(\infty)}{[c_s^2(\infty) + v(\infty)^2]^{3/2}}\left[\frac{2}{5 - 3\gamma}\right]^{\frac{5-3\gamma}{2(\gamma-1)}} \tag{2.45}$$

So the overall result is the same as our simple result from earlier, but the prefactors are right now and we can account for motion of the central body within the accreting medium.

There are, however, some limitations to this theory. There is some fine tuning required depending on the exact boundary conditions. In reality, shocks are expected. Secondly, this theory assumes no heat transport, which is likely not valid on long enough timescales. Thirdly, it is assumed that the accreting material does not radiate, which can become quite important at small distances. Finally, we've assume perfect spherical symmetry and zero angular momentum. Still, though, this basic theory gives us a simple view into the theory of accretion.

## 2.3 Interacting Binaries

The majority of high energy stellar-mass phenomena are interacting binaries. These include cataclysmic variables (CVs), Algol systems, W UMa, low mass X-Ray binaries, type Ia Supernovae. If we have two stars of mass $m_1$ and $m_2$, Kepler's third law tells us that their period is given by

$$P^2 = \frac{4\pi^2 a^3}{G(m_1 + m_2)} \tag{2.46}$$

where $a$ is the semi-major axis of the orbit. Given enough time, tidal forces will act to circularize the orbit, and if so, $a$ is just the simple separation between the two stars (where $e$, the eccentricity, vanishes). A schematic of such a binary is shown in Figure 3. Regarding the situation shown in

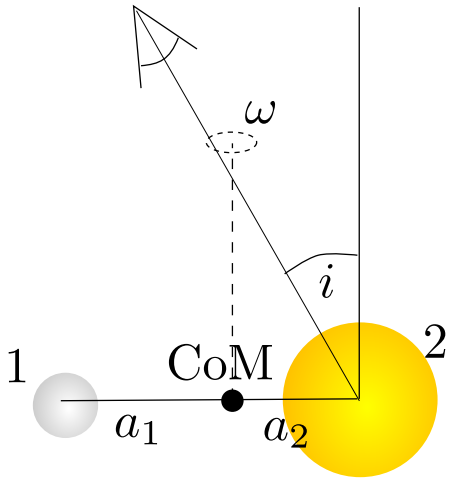


Figure 3: Schematic of an interacting binary. Stars 1 and 2 orbit about their center of mass as radii $a_1$ and $a_2$, respectively. An observer views this from an angle $i$ with $i = 0$ giving a face-on view and $i = 90°$ giving an edge-on view.

Figure 3, we have $a = a_1 + a_2$. Kepler's laws mandate $m_1 a_1 = m_2 a_2$. For convenience, we'll define $M = m_1 + m_2$. Then we can solve for an individual orbital radius of, say, star 1: $a_1/a = m_2/M$. If we can measure (spectroscopically or otherwise) the maximum velocity in the orbit, it will have first been modulated by our viewing angle. Specifically,

$$v_1 = v_{1,\mathrm{true}} \sin i = \left(\frac{2\pi}{P}\right) a_1 \sin i \tag{2.47}$$

for further convenience, we define the **mass function** via

$$f_1(m_1, m_2, i) \equiv \frac{(m_2 \sin i)^3}{(m_1 + m_2)^2} = \frac{P v_1^3}{2\pi G} \tag{2.48}$$

Define $q = m_1/m_2$ so that $M/m_2 = 1 + q$. Then the mass function becomes

$$f_1(m_2, i, q) = \frac{m_2(\sin i)^3}{(1+q)^2} \tag{2.49}$$

Using this all to solve for the semi-major axis $a$, we get

$$\boxed{a = 3 \times 10^{11} \text{ cm } \left(\frac{m_2}{M_\odot}\right)^{1/3} (1+q)^{1/3} P^{2/3}} \tag{2.50}$$

In general, $f_1 < m_2$ since $(\sin i)^3 \leq 1$ and $(1+q)^{-2} < 1$. If the source is double-lined, then we can measure velocities from both stars. In this case, the mass ratio is simply

$$q = \left(\frac{f_2}{f_1}\right)^{1/3} \tag{2.51}$$

### 2.3.1 Roche Potentials

To deal with the equipotential surfaces of such binaries, we first define the angular velocity vector, given by

$$\boldsymbol{\Omega} = \sqrt{\frac{GM}{a^3}}\,\hat{z} \tag{2.52}$$

In the co-rotating frame (where the stars are at rest), the potential has two terms: a gravitational potential and a centrifugal potential. The overall potential is then given by

$$\Phi = \Phi_G + \Phi_\Omega = -\frac{Gm_1}{|\mathbf{r} - \mathbf{r}_1|} - \frac{Gm_2}{|\mathbf{r} - \mathbf{r}_2|} - \frac{1}{2}(\boldsymbol{\Omega} \times \mathbf{r})^2 \tag{2.53}$$

Where here, the coordinate system has the center of mass of the binary at its origin and, again, it is co-rotating with the binary. Near each star, the potential is like the circular potential of the isolated star, and very far away, the potential is like that from a point source at the center of mass. In the intermediary stages, though, tear-dropped contours form for the equipotential surfaces. An example of such equipotential contours from a binary system is shown in Figure 4. There are three main configurations for a binary system with respect to these Roche potentials. A **detached** binary has both stars situated fully within their Roche lobes (within the potential with $L_1$ in it). A **semi-detached** binary has one star with a radius that exceeds its Roche lobe. Finally, a **contact binary** has both stars exceeding their Roche lobe, forming a "common envelope". $L_1$, or the inner Lagrange point, is a saddle point. That is, it is a point of quasi-stable equilibrium. It is a maximum in the potential in the $x-$direction and a minimum in the $y$-direction. If expansion proceeds beyond $L_2$ or $L_3$ (which are also saddle points), then mass is lost from the system. $L_4$ and $L_5$ are also local maxima and are thus unstable. These considerations also apply to non-stellar binaries like the Earth and the sun. For instance, WMAP is currently located at $L_2$, and JWST will (hopefully) soon join it. This allows them to be beyond Earth's shadow so they can use solar panels.

For now, let's assume $m_1 > m_2$, and define $R_1$, $R_2$ as the radii of spheres with the radius of the Roche lobe. Remember that $q = m_1/m_2$ (in our definition, it may vary depending on the book

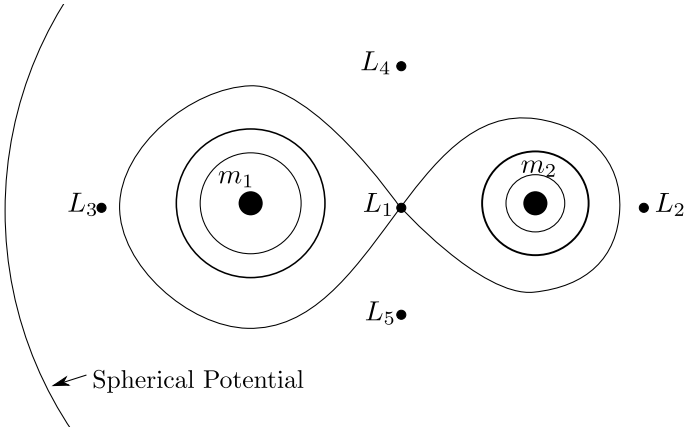


Figure 4: Equipotentials for a binary star system. Those contours closest to the stars resemble spherical potentials about an individual star, and those furthest away resemble contours from a point mass located at the center of mass. The intermediate regime shows distorted shapes resulting from competition between the two stars. Also shown are the Lagrange points as discussed in the text.

you are reading). Furthermore, define $b_1$ and $b_2$ to be the distances from each star to $L_1$. In 1983, Eggleton developed an approximation for the Roche lobe radius:

$$\frac{R_2}{a} = \frac{0.49q^{-2/3}}{0.6q^{-2/3} + \ln(1 + q^{-1/3})} \tag{2.54}$$

For example, if $q = 10$, then $R_2/a \approx 0.21$. If we instead wanted to write this explicitly in terms of the masses, then we get

$$\frac{R_2}{a} = 0.462 \left( \frac{m_2}{m_1 + m_2} \right)^{1/3} = 0.462 \, (1 + q)^{-1/3} \tag{2.55}$$

but only for the limited range $1.25 \leq q \leq 10$. This gives the same result for $q = 10$, though. There is also a semi-analytic approximation for $b_1$, which is the distance from $L_1$ to the primary, $m_1$:

$$\frac{b_1}{a} = 0.500 + 0.227 \log_{10} q \tag{2.56}$$

Now if we consider the case where $m_2$ is overflowing its own Roche lobe, we can calculate the average density inside the Roche lobe by using the orbital period:

$$\langle \rho_2 \rangle = \frac{3m_2}{4\pi R_2^3} = \frac{3}{4\pi (0.462)^3 a^3} M = \frac{\pi M}{4\pi^2 a^3} = \frac{\pi}{(0.462)^3 G P^2} \tag{2.57}$$

where we've used Kepler's law to eliminate the semi-major axis. Scaling this result, we get

$$\langle \rho_2 \rangle \sim 115 \left( \frac{P}{\text{hr}} \right)^{-2} \text{ g cm}^{-3} \tag{2.58}$$

So for binaries with a period of a few hours, those stars with mean densities typical of the lower main sequence with $\langle \rho \rangle \sim 1 - 100$ g cm$^{-3}$ can fill their Roche lobes.

### 2.3.2 Mass Transfer and Effects on Orbits

Before we concluded that for $i, j = 1, 2$ and $i \neq j$,

$$a_i = \frac{am_j}{M} \tag{2.59}$$

Now the total angular momentum, using the binary's angular frequency, $\omega = 2\pi/P$, is given by

$$J = m_1 a_1^2 \omega + m_2 a_2^2 \omega + I\omega_1 + I\omega_2 \tag{2.60}$$

where we are assuming that $I \ll a^2 m$ (the moment of inertia). Dropping those terms and eliminating the orbital radii in favor of masses and the overall semi-major axis, we can get

$$J = m_1 a_1^2 \omega + m_2 a_2^2 \omega \tag{2.61}$$

$$= \frac{m_2 m_1^2 a^2}{M^2}\omega + \frac{m_1^2 m_2 a^2}{M^2}\omega = \frac{a^2 m_1 m_2 M}{M^2}\omega \tag{2.62}$$

$$= \frac{m_1 m_2}{M} a^2 \omega \tag{2.63}$$

Now if we assume that no mass is lost and no angular momentum is lost (essentially assuming a stream of matter between the two stars with no mass lost along the way), then we have $\dot{m}_1 = -\dot{m}_2$ and $\dot{J} = 0$. The effect this has on the period is then

$$\frac{\dot{P}}{P} = \frac{3\dot{M}(m_1 - m_2)}{m_1 m_2} \tag{2.64}$$

So if the heavier star losses mass, the period decreases, and since $P \propto a^{3/2}$, the orbital separation must also decrease, causing runaway mass transfer (since the Roche lobe shrinks as mass is lost). On the other hand, if the lighter star loss mass, both the period and the orbital separation will increase.

Often a fraction of the mass lost from one star will be completely lost from the system. This is a common consequence of spherical mass winds. This is called non-conservative mass loss. Let's assume for now that $\dot{m}_1 = 0$ but $\dot{m}_2 \neq 0$. Then the angular momentum loss is

$$\dot{J} = \dot{m}_2 a_2^2 \omega \tag{2.65}$$

and the orbital separation and period both increase according to

$$\frac{\dot{a}}{a} = -\frac{\dot{m}_2}{M} \qquad \Rightarrow \qquad \frac{\dot{P}}{P} = -\frac{2\dot{m}_2}{M} \tag{2.66}$$

# 3 White Dwarfs

The first discovered white dwarf (WD) was discovered in 1783 by William Herschel. It was discovered in a triple system consisting of 40 Eri A, 40 Eri B, and 40 Eri C. 40 Eri B was the WD what was observed, though it was not well understood at the time. Much later in 1914, Russel (of the Herzprung-Russel diagram) identified the spectrum of 40 Eri B as an A star (taken in 1910). Note that 40 Eri B is not the closest WD, but it is the most easily observed.

The next WD discovered was Sirius B, which was suspected astrometrically by Bessel as early as 1844. This is because there was an observed departure from linear motion of Sirius A (the really bright star). He wrote in 1844

> The existence of numberless visible stars can prove nothing against the existence of numberless invisible ones.

Sirius B was first observed in 1862 by Alvan Graham Clark, and in 1915, Walter Adams obtained a spectrum, declaring that it was both faint and white. Later in 1928, he detected a gravitational redshift in this spectrum, which was actually the first test of GR. He concluded that it was 2000 times denser than platinum.

In 1927, Eddington mused about Sirius B

> The message of Sirius, when it was decoded ran, "I am composed of material 3,000 times denser than anything you have ever come across; a ton of my material would be a little nugget you could put in a match box." What reply can be made of a such a message? The reply most of us made in 1914 was, "Shut up. Don't talk nonsense."

It wasn't until 1917 that the first isolated WD was discovered van Maanan's star. No new ones were discovered until the 1930's.

## 3.1 Observed Properties of WDs

We can break WDs up into classes according to different spectroscopic properties. Each of the classes begin with a "D", designating dwarf.

- DA stars show strong hydrogen lines. These constitute about 2/3 of all WDs.
- DB stars show strong He I lines, making up about 8% of all WDs.
- DO stars show strong He II lines, making up about 14% of all WDS.
- DC stars show no strong lines and are relatively rare ($\sim 1\%$)
- DZ stars show strong metal lines but no carbon. These are also pretty rare.
- DQ stars show strong carbon lines, and they make up about 0.1% of all WDs.

These spectroscopic classes also show variety in their effective temperatures. DO stars have $T_{\text{eff}} \approx 100,000\text{ K} - 45,000\text{ K}$. DB stars are a bit cooler at $30,000\text{ K} - 12,000\text{ K}$. DC stars are even cooler, typically less than $12,000$ K. DQ stars are typically warmer than 15,000 K.

The typical mass of a WD is around $0.5 - 0.6\ M_\odot$ with surface gravities of around $\log g \approx 8.0$. Some of these are variable. ZZ Ceti variables are WDs with $T_{\text{eff}} \approx 12,000$ K with pulsational periods of $P \sim 100 - 1000$ s. There are also variable DA stars (DAVs) that exhibit nonradial pulsations that are driven by partial ionization of the hydrogen in their atmospheres. DBV stars act similarly due to partial helium ionization zones at $T_{\text{eff}} \sim 27,000$ K. There are also planetary nebula variables (PNNVs) that are present right after the birth of a WD.

Most WDs are largely composed of carbon and oxygen (C-O WDs), though there are also lower-mass pure He WDs. On the higher end of the mass scale, there are Oxygen-Neon (O-Ne) WDs, but most have hydrogen in their atmospheres. Due to the intense surface gravity, there is thorough surface stratification. That is, there is nearly pure hydrogen on the surface with heavier elements sinking to the lower levels. As a result, DA WDs dominate the population since even a small amount of hydrogen will form a nearly pure layer at the top.

## 3.2 White Dwarf Structure

We'll begin by discussing some macroscopic equations governing pressure and density in white dwarfs. Recall that a white dwarf is just the degenerate core of an old star that is so dense that the pressure is due nearly entirely to electron degeneracy pressure. As a result of this, pressure is independent of temperature. Mass conservation tells us that

$$dm(r) = 4\pi r^2 \rho(r) \tag{3.1}$$

and hydrostatic balance mandates that

$$\frac{dP(r)}{dr} = -\frac{Gm(r)\rho(r)}{r^2} \tag{3.2}$$

We also want a relationship between the pressure $P$ and the density $\rho$. We'll assume a polytropic equation of state

$$P = K\rho^{\gamma} = K\rho^{1+1/n} \tag{3.3}$$

where $n$ is the polytropic index. The microscopic properties will give us the polytropic index or $\gamma$ more precisely, but now we'll present a rough derivation as given by Landau.

### 3.2.1 Equations of State

Consider a uniform density of fermions (say, electrons). Define the number density as

$$n = \frac{3N}{4\pi R^3} \tag{3.4}$$

where $R$ is the size of the star. The average spacing of the particles is then $\Delta x \approx n^{-1/3}$. Heisenberg's uncertainty principle tells us

$$\Delta x \Delta p \sim \hbar \qquad \Rightarrow \qquad \Delta p \sim \frac{\hbar}{\Delta x} \approx \hbar n^{1/3} \tag{3.5}$$

Then the total energy, relativistically speaking, is

$$E^2 = p^2c^2 + m^2c^4 \tag{3.6}$$

If we assume $pc > mc^2$ (the ultra-relativistic limit), we get an internal energy of (using our momentum relation from above)

$$E_i \approx pc = \hbar c \left(\frac{3N}{4\pi R^3}\right)^{1/3} = \hbar c \left(\frac{3}{4\pi}\right)^{1/3} \frac{N^{1/3}}{R} \tag{3.7}$$

The gravitational energy per fermion of such a uniform density ball would be

$$E_g = -\frac{3GM}{5R} \tag{3.8}$$

where $M = Nm_{\text{particle}}$. The the total energy (the sum of the two) is

$$E_{\text{tot}} = E_i + E_G = \frac{1}{R}\left(\hbar c\left(\frac{3}{4\pi}\right)^{1/3} N^{1/3} - \frac{3}{5}GNm_{\text{particle}}\right) \tag{3.9}$$

We find equilibrium when there is no energy gradient, $\partial E/\partial r = 0$ when the right hand side vanishes:

$$\left(\frac{3}{4\pi}\right)^{1/3} N^{1/3}\hbar c = \frac{3}{5}GNm_{\text{particle}} \tag{3.10}$$

$$N^{2/3} = \frac{\left(\frac{3}{4\pi}\right)^{1/3}\hbar c}{\frac{3}{5}Gm_{\text{particle}}} \tag{3.11}$$

$$N_{\text{critical}} = \frac{\left(\frac{3}{4\pi}\right)^{1/2}(\hbar c)^{3/2}\left(\frac{5}{3}\right)^{3/2}}{G^{3/2}m_{\text{particle}}^{3/2}} \tag{3.12}$$

$$= \left(\frac{3}{4\pi}\frac{5}{3}\right)^{1/2}\frac{5}{3}\left(\frac{\hbar c}{Gm_{\text{particle}}}\right)^{3/2} \tag{3.13}$$

$$= \frac{5\sqrt{5}}{6\sqrt{\pi}}\left(\frac{\hbar c}{Gm_{\text{particle}}}\right)^{3/2} \tag{3.14}$$

$$= 2.3 \times 10^{57}\,\text{particles} \tag{3.15}$$

The corresponding mass is

$$M_{\max} = N_{\text{crit}} * m_{\text{particle}} = 1.05\left(\frac{\hbar c}{G}\right)^{3/2} m_{\text{particle}}^{-2} \sim 1.9\,M_\odot \tag{3.16}$$

There have made a lot of approximations here, so now we'll do a more detailed calculation. What's interesting to note, though, is that quantum mechanics, gravitational potential, and electromagnetism were enough to specify the macroscopic mass of the object. If the WD is larger than this, the energy is negative, causing collapse (making this a maximum possible mass attainable by a WD in equilibrium). If it is smaller, then the radius would increase until equilibrium is reached.

We'll still assume that the average spacing between particles is given by $\Delta x \sim n^{-1/3}$. For degeneracy pressure to be the dominant source of support, we must be in the regime where

$$\Delta pc \gg kT \tag{3.17}$$

We can effectively treat our white dwarfs as as zero temperature objects then, since kinetic pressure is negligible. Fermi-Dirac statistics give a number density (in phase space) of

$$\frac{dN}{d^3x\,d^3p} = \frac{g}{\hbar^3}\underbrace{\frac{1}{e^{(E-\mu)/kT}+1}}_{f(E)} \tag{3.18}$$

Here, $g$ is a statistical weight that, for electrons is 2 due to the two spin states of the electron. $E$ is the particle energy and $\mu$ is the chemical potential. When quantum effects are unimportant, $f(e) \approx \exp(\mu - E)/(kT)$, and the distribution function resembles that of a Maxwell-Boltzmann distribution. At lower temperatures, though, $f(E)$ resembles a step function:

$$f(E) = \begin{cases} 1 & : E \leq E_F \\ 0 & : E > E_F \end{cases} \tag{3.19}$$

where $E_F$ is the Fermi Energy, which is the chemical potential at $T = 0$. There is a momentum associated with this energy, given by

$$E_F = \left(p_F^2 c^2 + m_e^2 c^4\right)^{1/2}. \tag{3.20}$$

Now we wish to find the number density, which requires we integrate the distribution function over all momenta:

$$\frac{N}{d^3x} = n_e = \int_0^\infty dn = \frac{2}{h^3}\int_0^{p_F} 4\pi p^2\, dp \tag{3.21}$$

This gives a number density of

$$n_e = \frac{8\pi}{3h^3} p_F^3 \tag{3.22}$$

Now solving for the Fermi momentum,

$$p_F = \left(\frac{3h^3}{8\pi} n_e\right)^{1/3} \tag{3.23}$$

Now we can relate the electron number density to the overall mass density via

$$n_e = \frac{Y_e \rho}{m_{\rm B}} \tag{3.24}$$

where $Y_e$ is the number of electrons per nucleon (typically around a half for a C-O WD due to neutrons). Then the Fermi momentum is

$$p_F = \left(\frac{3h^3 Y_e \rho}{8\pi m_{\rm B}}\right)^{1/3} \propto \rho^{1/3} \tag{3.25}$$

Now we'll look at some limiting regimes. In the nonrelativistic case, we can assume that $p_F \ll m_e c$ and $E_F \approx m_e c^2$. For the relativistic case, $p_F \gg m_e c$ and $E_F \approx pc$. Back to our equation of state, $P = K\rho^\gamma$, we'll find that in the nonrelativistic limit, $\gamma = 5/3$, but in the relativistic regime, $\gamma = 4/3$. We'll now show where these number come from.

First, though, we need to revisit the general relation between pressure and energy density, which we'll denote as $\mathcal{E}$. The general relation is

$$P = (\gamma - 1)\mathcal{E} \tag{3.26}$$

This $\gamma$ is the same as before, and is the adiabatic $\gamma$, the ratio of specific heats, $\gamma = c_P/c_V$. Now let's use this relation to investigate degeneracy in the nonrelativistic limit. The kinetic energy of a nonrelativistic electron is

$$E = \frac{1}{2} m_e v^2 = \frac{1}{2} m_e \left(\frac{p^2}{m_e^2}\right) = \frac{p^2}{2m_e} \tag{3.27}$$

Assuming a characteristic spacing distance of $\Delta x = a$, or $a = (m_p/\rho)^{1/3}$ this corresponds to

$$E \approx \frac{\hbar^2}{2m_e a^2} \tag{3.28}$$

The energy density then is

$$\mathcal{E} = E/a^3 \approx \frac{\hbar^2}{2m_e a^5} \tag{3.29}$$

Putting this in terms of the density, we get

$$\mathcal{E} = \frac{\hbar^2}{2m_e}\left(\frac{\rho}{m_{\rm B}}\right)^{5/3} \tag{3.30}$$

Here we've already shown that $\gamma = 5/3$, but we will use the pressure-energy density relation to get

$$P = \frac{\hbar^2}{3m_e}\left(\frac{\rho}{m_{\rm B}}\right)^{5/3} \tag{3.31}$$

A more careful derivation would give a pressure of

$$\boxed{P_{\rm non-rel} = \frac{(3\pi^2)^{2/3}}{5}\frac{\hbar^2}{m_e}Y_e^{5/3}\left(\frac{\rho}{m_e}\right)^{5/3}} \tag{3.32}$$

Fantastic. Now let's investigate the relativistic case, where $E \approx pc \approx hc/a$ (via Heisenberg Uncertainty Principle again). Then the energy density is

$$\mathcal{E} = \frac{E}{a^3} \approx \frac{hc}{a^4} = hc\left(\frac{\rho}{m_p}\right)^{4/3} \tag{3.33}$$

So now we see that $\gamma = 4/3$ in the relativistic case. Converting this to pressure in a more detailed calculation gives

$$\boxed{P_{\rm rel} = \frac{(3\pi^2)^{1/3}\hbar c Y_e^{4/3}}{4}\left(\frac{\rho}{m_{\rm B}}\right)^{4/3}} \tag{3.34}$$

### 3.2.2 Mass-Radius Relation for White Dwarfs

Linearizing the equation for hydrostatic equilibrium, (3.2), we find

$$\frac{P}{r} \sim \frac{m(r)\rho}{r^2} \sim r\rho^2 \tag{3.35}$$

Now mandating that $P \propto \rho^\gamma$, this gives us

$$\rho^\gamma \sim r^2\rho^2 \qquad \Rightarrow \qquad \rho \sim r^{2/(\gamma-2)} \tag{3.36}$$

Now assuming $M \sim \rho r^3$, we find

$$M \sim r^{\frac{3\gamma-4}{\gamma-2}} \tag{3.37}$$

So we see that as $\gamma \to 5/3$, we find

$$R \propto M^{-1/3} \tag{3.38}$$

and for the relativistic case ($\gamma = 4/3$), we find that mass is independent of radius!

## 3.3 The Chandrasekhar Mass

*Monday, April 22, 2013*

We'll only use the first two equations of stellar structure:

$$\frac{dP}{dr} = -\frac{GM(r)\rho(r)}{r^2} \qquad \frac{dM}{dr} = 4\pi r^2 \rho \tag{3.39}$$

Now we'll assume a polytropic equation of state, $P = K\rho^\gamma$ to combine these two equations and eliminate $P$ in favor of $\rho$:

$$\frac{d}{dr}\left(\frac{r^2}{\rho}\frac{dP}{dr}\right) + 4\pi G\rho r^2 = 0 \tag{3.40}$$

We now change variables to

$$w = \left(\frac{\rho(r)}{\rho_c}\right)^{1/n} \tag{3.41}$$

where $\gamma = 1 + 1/n$. Additionally, we'll express the radial coordinate as $r = az$ where

$$a = \left[\frac{(n+1)K\rho_c^{1/n-1}}{4\pi G}\right]^{1/2} \tag{3.42}$$

and $z$ is a dimensionless distance. With that witchcraft behind us, eq. (3.40) becomes the **Lane-Emden Equation**:

$$\frac{1}{z^2}\left[\frac{d}{dz}\left(z^2\frac{dw}{dz}\right)\right] + w^n = 0. \tag{3.43}$$

This equation, in general, cannot be solved analytically, though we can sketch a general set of solutions. Solving the mass equation with this density solution, we get

$$M = 4\pi\rho_c \int_0^R w^n r^2\, dr = 1.437\, M_\odot\, (2Y_e)^2 \tag{3.44}$$

where the second expression is in the relativistic limit, i.e., the Chandrasekhar Mass. The radial coordinate is then

$$R = 3.347 \times 10^9 \left(\frac{\rho_c}{10^6\ \mathrm{g/cm^3}}\right)^{-1/3} (2Y_e)^{3/2}\ \mathrm{cm} \tag{3.45}$$

for the nonrelativistic case and

$$R = 1.122 \times 10^9 \left(\frac{\rho}{10^6\,\mathrm{gm/cm^3}}\right)^{-1/6} (2Y_e)^{5/6}\ \mathrm{cm} \tag{3.46}$$

for the relativistic case. We can express the nonrelativistic mass in terms of the central density or the radius via

$$M(\rho_c) = 0.4964 \left(\frac{\rho_c}{10^6\,\mathrm{g/cm^3}}\right) 61/2\, (2Y_e)^{1/2}\ M_\odot \tag{3.47}$$

$$M(R) = 0.7011 \left(\frac{R}{10^9\,\mathrm{cm}}\right)^{-3} (2Y_e)^5\ M_\odot \tag{3.48}$$

## 3.4 White Dwarf Cooling

Typically a WD isn't just a ball of degenerate matter. There is usually a very thin (by mass) layer of nondegenerate H/He that actually dominates the cooling process of the WD. This is much how the luminosity able to exit a star sets the rate at which fusion occurs at the center. Before we press on, here are some fun facts about WDs. 97% of stars will end up as WDs. That is, 97% of stars are less than 8 $M_\odot$. The peak in the WD mass function is around 0.6 $M_\odot$, so we would expect to see a lot of WDs near that mass.

So the H/He layer is an optically thick insulating layer that keeps the underlying WD hot. The interior is largely isothermal due to the efficiency of heat transport by electrons, and is supported by electron degeneracy. An understanding of the WD cooling process, we must first understand the luminosity of the WD (that is, the rate at which it is losing thermal energy since there is no nuclear energy to power the WD). Radiative diffusion tells us that

$$L = -4\pi r^2 \frac{c}{3\kappa\rho}\frac{d}{dr}\left(aT^4\right) \tag{3.49}$$

where $a$ is the radiation constant (it's nasty, but built from fundamental constants). $(\kappa\rho)^{-1}$ is the mean free path of photons diffusing through medium, with $\kappa$ being the opacity, with dimension of area per mass (essentially the cross section per unit mass). Simply carrying through the derivative, we get

$$L = -16\pi r^2 \frac{acT^3}{3\kappa\rho}\frac{dT}{dr} \tag{3.50}$$

Solving for the temperature gradient, we get

$$\frac{dT}{dr} = -\frac{3\kappa\rho}{4acT^3}\frac{L}{4\pi r^2} \tag{3.51}$$

If we assume a Kramers' Law dominates the opacity (where $\kappa \propto \rho T^{-3/2}$), we can get a more precise handle on this. For now we'll assume the following parameters

$$\kappa_0 = 4.31 \times 10^{24} Z(1+X)\,\mathrm{cm}^2\,\mathrm{g}^{-1} \tag{3.52}$$

$$\tag{3.53}$$

where $\kappa = \kappa_0 \rho T^{-3/2}$. Now, because we know where we're going, we do some bizarre math, where we divide the condition for hydrostatic equilibrium by the temperature gradient to give us $dP/dT$:

$$\frac{dP}{dr} = -\frac{GM(r)\rho(r)}{r^2} \qquad \Rightarrow \qquad \frac{dP}{dT} = \frac{16\pi acGMT^{-6.5}}{3\kappa_0 L\rho} \tag{3.54}$$

where we've approximated $M(r) \approx M$ in the outermost layers of the WD. We can eliminate $\rho$ by using the relation between pressure, density, and temperature. We will assume an ideal gas equation of state to do so, meaning that $\rho = P\mu m_\mathrm{B}/(kT)$. This gives us

$$P\,dP = \frac{16\pi acGMk}{3\kappa_0 L\mu m_\mathrm{B}} T^{7.5}\,dT \tag{3.55}$$

Integrating this from the surface inwards, we get

$$\int_0^P p\,dp = \mathcal{G}\int_0^T \tau^{7.5}\,d\tau \tag{3.56}$$

where we're assuming a $P = T = 0$ boundary condition at the "surface", and $\mathcal{G}$ holds all those stupid constants. The resulting equation relating density to temperature is

$$\boxed{\rho = \left(\frac{64\pi acGM\mu m_{\rm B}}{51\kappa_0 Lk}\right) T^{13/4}} \tag{3.57}$$

Gross, right? Now at some point, the density is high enough so that the matter becomes degenerate and these approximations fail. At this point, $T_* \sim T_c$ due to the isothermal nature of degenerate material. Additionally,

$$\frac{\rho_* kT_*}{\mu_e m_{\rm B}} = 1.0\times 10^{13}\left(\frac{\rho_*}{\mu_e}\right)^{5/3} \tag{3.58}$$

where $\mu_e = 1/Y_e$. This is essentially stating that the pressure due to an ideal gas (the LHS) is equation to that from degenerate electrons (the RHS). We can solve for this critical density at which degeneracy takes over to find

$$\rho_* \approx 48\,\mathrm{g\,cm^{-3}}\left(\frac{\mu_e}{2}\right)\left(\frac{T_*}{10^6\ \mathrm{K}}\right)^{3/2} \tag{3.59}$$

Now solving for the luminosity as a function of the core temperature, we find

$$L = 1.43\times 10^{-7}\,L_\odot\,\frac{\mu}{\mu_e}\frac{1}{Z(1+X)}\left(\frac{M}{M_\odot}\right)\left(\frac{T_c}{10^6\,\mathrm{K}}\right) \tag{3.60}$$

Or more succinctly, $L = CMT_c^{7/2}$ where $CM_\odot = 2\times 10^6$ erg/s. Now we might ask what the characteristic cooling time is. What is the timescale on which the temperature will change significantly? If we have the luminosity, we should also figure out what the thermal energy of the WD is, since that is what is initially being radiated away, though crystallization energy losses eventually become important. Assuming ideal gas internal energy, the thermal energy is approximately

$$E_{\rm thermal} = \frac{3}{2}NkT_c = \frac{3}{2}\left[\frac{M}{23m_{\rm B}}\right]kT_c \tag{3.61}$$

assuming pure carbon-12 in the core. A typical energy at birth would be about $E_{\rm birth}\sim 10^{58}$ ergfor a 0.4 $M_\odot$ WD at $T_c \sim 10^8$ K. Assuming that the luminosity is the time rate of change of the thermal energy, or

$$-\frac{dE}{dt} = L \qquad \Rightarrow \qquad \frac{3}{2}\frac{km}{Am_{\rm B}}\frac{dT_c}{dt} = CMT_c^{7/2} \tag{3.62}$$

(where $A$ is the average mass number of core material.) Integrating, we find

$$\frac{3}{5}\frac{k}{Am_{\rm B}}\left(T^{-5/2} - T_0^{5/2}\right) = C(t-t_0) \tag{3.63}$$

For some constant $C$. If we assume that at early times, $T_0 \gg T$ and defining $t_0 = 0$, we get

$$\frac{3kT^{-5/2}}{5Am_{\mathrm{B}}} \approx Ct \tag{3.64}$$

Solving for this time, we get

$$t = \frac{3kMT}{5Am_{\mathrm{B}}L} \tag{3.65}$$

Parameterizing this result, we have

$$t \approx 10^8 \text{ yrs } A^{-1} \left(\frac{M/M_\odot}{L/L_\odot}\right)^{5/7} \tag{3.66}$$

## 3.5 Cataclysmic Varaiables

*Wednesday, April 24, 2013*

A **cataclysmic variable** (CV) is a binary system typically consisting of either a main sequence (MS) or red giant (RG) and a white dwarf (WD) with the MS/RG star overflowing its Roche lobe (RLOF for Roche Lobe OverFlow) and donating matter to the WD. These binaries typically have periods of 80 minutes to several hours. CVs give off radiation from several sources

- Secondary (MS/RG)
- Accretion Disk
- Bright spot where accreted material hits disk
- WD surface

Different sources are relevant for different types of CVs, which we'll now summarize.

### 3.5.1 Classical Novae

A classical nova (CN) has a rapid rebrightening of 6 to 19 magnitudes in the optical. We only see one of these outbursts (as opposed to a recurrent nova, which we'll discuss later). Our current understanding of what causes these events is the accumulation of hydrogen on a WD, followed by ignition at the base in degenerate conditions. As the hydrogen burns to helium, the temperature grows at constant pressure (due to the degenerate nature of the material, which doesn't care about the temperature). This causes a runaway which results in removing a lot of the hydrogen-rich material. We expect there to be about 30 of these each year in the Milky Way, though we may not see most of them due to dust extinction.

During an outburst, CNe reachs the Eddington luminosity, at which point the hydrogen rich material is blown off of the surface with wind velocities on the order of 1000 km/s over a timescale of days to weeks. Recall that the Eddington luminosity

$$L_{\mathrm{Edd}} \sim 1.34 \times 10^{38} \left(\frac{M}{M_\odot}\right) \text{ erg s}^{-1} \sim 10^{38} \text{ erg s}^{-1} \tag{3.67}$$

Then the total radiated energy is approximately

$$E_{\rm tot} = L_{\rm Edd}\Delta t \sim 10^{45}\ {\rm erg} \tag{3.68}$$

which corresponds to approximately $10^{-7}\ M_\odot$ of hydrogen burned to helium. At an accretion rate of $\dot{M} \sim 10^{-10}\ M_\odot/{\rm yr}$, we would expect these to go off about every 1000 years (so not recurrent on our timescales).

### 3.5.2 Recurrent Novae

Recurrent novae are very similar to classical novae, but they reoccur on timescales of decades. These explosions are less violent, causing less mass loss. This is likely because the ignition takes place when the material is still nondegenerate.

### 3.5.3 Dwarf Novae

A dwarf novae is a rebrightening of around 2 to 5 magnitudes, thought to be linked with accretion. An instability in the accretion disk causes a short increase in the accretion rate, resulting in an increase in brightness. These events can occur with recurrence times on the order of days to weeks or longer. A dwarf nova (while active) has a luminosity of approximately $L \sim 10^{34}\ {\rm erg\ s^{-1}}$.

### 3.5.4 Magnetic CVs

Magnetic CVs are accreting WDs with very strong magnetic fields ($\sim 10^7$ Gauss) where the accreted matter is funneled to the magnetic poles. They have a high state and a low state of emission. A classic example of these is T Cor Bor, which consists of a giant and a magnetized WD, which exhibits recurrent high states.

### 3.5.5 General Considerations

Let's look at the orbital dynamics of such system. Kepler's Third Law (with some sensible scaling) is

$$a = \left(3.5 \times 10^{10}\ {\rm cm}\right)\left(\frac{P}{\rm hr}\right)^{2/3}\left(\frac{M}{M_\odot}\right)^{1/3} \tag{3.69}$$

For reference, a solar radius is $R_\odot = 7 \times 10^{10}$ cm and for a WD, $R_{\rm WD} \sim 5 \times 10^8$ cm, so these are very tight binaries!

At the innermost region of an accretion disk, there is a boundary layer where the material first "enters" the WD. From the virial theorem, we can assume that the material passing through this boundary layer has half of its energy radiated away and half enters the star as heat. The accretion luminosity is

$$L = \frac{GM_{\rm WD}\dot{M}}{R_{\rm WD}} \tag{3.70}$$

Half of this is radiated away and appears as radiation from the disk

$$L_{\rm disk} = L_{\rm BL} \sim \frac{GM_{\rm WD}\dot{M}}{2R_{\rm WD}} \tag{3.71}$$

If we assume some characteristic values of $R_{\rm WD} = 6 \times 10^8$ cm, $M_{\rm WD} = M_\odot$, and $\dot{M} = 1.6 \times 10^{-10}\ M_\odot$ yr, we get an accretion luminosity of $L \sim 10^{33}$ erg s$^{-1}$. Assuming a perfect blackbody is generating this luminosity (and that the energy is radiating away from both sides of the disk), we can use the Stefan-Boltzmann law to solve for a characteristic temperature:

$$2\pi R_{\rm disk}^2 \sigma T_{\rm out}^4 \approx \frac{GM_{\rm WD}\dot{M}}{R_{\rm WD}} \tag{3.72}$$

Using $R_{\rm disk} = 4 \times 10^{10}$ cm and our previous assumptions, we get $T_{\rm disk} \approx 2 \times 10^3$ K.

Now, if all of the radiation comes from the inner radius, the above analysis must be adjusted to reflect $R_{\rm disk} \to R_{\rm WD}$. This results in a temperature of $T_{\rm max} \approx 5 \times 10^4$ K. So the range of temperatures is $10^3 - 10^5$ K , and it would radiate primarily in the visible to ultraviolet. In reality, the bounding layer can be smaller than $2\pi R_{\rm WD}^2$ if it is an annulus which causes the temperature to go even higher into the extreme UV or soft X-Rays.

In magnetic WDs, the flux is channeled to a small polar cap $\sim$ 10 km with ree-fall velocities, so the temperatures can be as high as $T \sim 10^8$ K ($\sim$10 keV). There may also be circularly polarized radiation at cyclotron frequencies of

$$\nu = \frac{eB}{m_e c} = 2.8 \times 10^{13}\ \text{hz}\ \left(\frac{B}{10^7\ \text{G}}\right) \tag{3.73}$$

which is in the near IR. This radiation would be absorbed by the WD and re-radiated in the EUV to optical ranges. A spectrum from a CV will have low frequency components from a companion red star, medium frequency components from an accretion disk, and/or high frequency components from the boundary layer where the material meets the WD.

# 4 Neutron Stars

Neutron stars were first discovered in 1967 by Jocelyn Bell and Hewish (Hewish later got a Nobel prize). They discovered pulsars through radio observations, originally thinking they might be aliens. After discovering several of these LGMs (Little Green Men), they concluded that they were not, in fact, aliens, but some astrophysical object.

When a WD's mass exceeds the Chandrasekhar mass, it will begin to collapse as the pressure from degenerate electrons can no longer halt the gravitational force. This can also occur in a degenerate core of a massive store (like an iron core). Note that this is *not* what causes a Type Ia supernova. Those start when a C-O WD *approaches* $M_{\rm Ch}$, triggering explosive carbon burning. *Exceeding* $M_{\rm Ch}$ results in collapse to a neutron star.

At some point, the electrons' Fermi energy,

$$E_{\rm F}(e^-) = \sqrt{(p_{\rm F}c)^2 + (m_e c^2)} \tag{4.1}$$

exceeds

$$(m_n - m_p)c^2 = 1.29 \text{ MeV} \tag{4.2}$$

This happens at a density of $\rho_0 = 1.2 \times 10^7$ g cm$^{-3}$. At higher densities, it becomes energetically favorable for electrons to inverse beta decay:

$$e^- + p \rightarrow n + \nu_e \tag{4.3}$$

This leads to more and more neutrons and, ultimately, a neutron star.

More realistically, the WD contains nuclei (C and O, or O and Ne, etc.) and not free neutrons, protons, and electrons. Electrons capture onto nuclei to form increasingly neutron-rich nuclei. At a density of $\rho \approx 4.3 \times 10^{11}$ g cm$^{-3}$ neutrons begin to bleed from nuclei. This process is called "neutron drip" which "softens" the equation of state. The star continues to collapse until $\rho > 10^{14}$ g cm$^{-3}$, at which point neutron degeneracy pressure becomes strong enough to halt further compression. Note that normal nuclear matter (that is, nuclei) has a density of $\rho_{\rm nuc} \approx 2.8 \times 10^{14}$ g cm$^{-3}$. The equation of state at these high densities is highly uncertain and is sensitive nuclear theory.

The actual structure of a neutron star is a bit of a mystery, but if it is indeed just bare neutrons (it probably isn't), we can get some intuition from nuclear physics. The actual equation of state in a neutron star is highly uncertain. The radius of a nucleus is approximately given by $R_{\rm nuc} \sim A^{1/3}$ where $A$ is the mass number. The "radius" of a nucleon is $r_0 = 1.25$ fm $= 1.25 \times 10^{-13}$ cm, so the density of such nuclear matter is $\rho_{\rm nuc} = 3A^{1/3} m_n / (4\pi R_{\rm nuc}^3)$.

## 4.1 Relativistic Caveats

The Schwarzschild radius for a 1.4 $M_\odot$ black hole is about 3 km, so the general relativistic corrections are important in neutron stars, on the order of 20%. The Schwarzschild radius is

$$R_{\rm Sch} = \frac{GM}{c^2} \tag{4.4}$$

so we expect to see gravitational redshifts of

$$\frac{GM}{c^2 R} \sim \frac{\Delta\lambda}{\lambda} = z \approx 0.2 \tag{4.5}$$

Such deviations in spectra are indeed observed in known neutron stars. As a result of general relativistic corrections, the standard equation of hydrostatic equilibrium is no longer valid. Instead, we must use the TOlman-Oppenheimer-Vokoff (TOV) equation, which is derived from assuming a spherically symmetric metric (and nearly nothing else!) in general relativity.

At masses above $M = M_\odot$, (and densities above nuclear densities), the equation of state breaks down. This adds an additional uncertainty to the mass-radius relation since things like nucleon-nucleon repulsion might soften the equation of state, but if new particles are created at high densities, this too might soften the equation of state. A softer equation of state means that there is a lower maximum mass. The mass limit for neutron stars is highly uncertain. We typically think it is somewhere around 2 $M_\odot$ to 3.2 $M_\odot$. Most neutron star masses are clustered around 1.4 $M_\odot$.

## 4.2 Neutron Star Structure

The general picture of a neutron star consists of an atmosphere, an outer crust, an inner crust, and outer core, and an inner core. The outer parts are fairly well understood, but as we move inwards, less and less is known. From the atmosphere through both crusts, it is estimate that about 1% of the mass is accounted for. The rest is in the core material.

**Atmosphere** At a temperatures of about $3 \times 10^6$ K, this is about 10 cm thick, and for temperatures of about $3 \times 10^5$ K, about 10 mm thick. We don't really understand the atmosphere with magnetic fields with $B > 10^{11}$ G or temperatures $T < 10^6$ K. Typically the density follows $\rho \leq 10^6$ g cm$^{-3}$ and the total mass in the atmosphere is negligible and comprised largely of $^{56}$Fe. This atmosphere shapes the emerging spectrum and contains a plasma layer that is highly ionized. The atomic energy levels are significantly distorted by the magnetic fields. For $B \sim 10^{12}$ G, atoms are shaped like needles. These weirdly-shaped atoms are the reasons why the atomic levels are distorted.

**Outer Crust** The outer crust is basically white dwarf material. The densities range from the atmospheric density up to $\rho \sim 14 \times 10^{11}$ g cm$^{-3}$. It is on the order of 100 m thick, and at the top, the dominant nucleus if $^{56}$Fe. There are non-degenerate to degenerate electrons present, and at high depths, the material is solid. Electron capture onto nuclei occurs, causing neutron drip at the bottom of the crust which forms a neutron gas with density $\rho \sim 4 \times 10^{11}$ g cm$^{-3}$.

**Inner Crust** The inner crust is approximately 1 km thick. The densities range from $\rho_{\text{drip}}$ to $0.5\rho_{\text{nuc}}$, where you may recall that $\rho_{\text{nuc}} \approx 2.8 \times 10^{14}$ g cm$^{-3}$. The matter consists of electrons, free neutrons, and neutron-rich nuclei. The preferred nucle become more and more neutron as the density is increased. The nucleon number reaches several, unlike on Earth. These nuclei are just no possible in pretty much any other place in the universe. However, the nuclei number goes to zero at the core boundary as the nuclei get distorted into strange shapes. This gives rise to the colorful terminology of nuclear pasta. Spherical nuclei are called meatballs, long thin nuclei are spaghetti, and nuclear slabs are called lasagna. There are also lattice inverts, which are voids embedded in nuclear matter, called swiss chese. Finally, there are touching nucleons touching, forming a uniform nuclear fluid (the "sauce"). It may be that this nucleon fluid is a superfluid at low temperatures, which would result in a vanishing viscosity in the fluid. The equation of state is relatively well-known for the crust.

**Outer Core** Here the density ranges from $0.5\rho_{\text{nuc}} < \rho < 2\rho_{\text{nuc}}$, and the neutron to proton ratio is approximately $n/p > 20$. Nuclei essentially cease to exist and the matter transitions to a neutron-proton fluid with negatively charged stuff. In this regime, nucleon-nucleon repulsion becomes important, and the neutrons become superfluid. Along with the inner core, this contains 99% of the mass.

**Inner Core** Here the densities are greater than $\rho \geq 2\rho_{\text{nuc}}$ and possibly as high as $10 - 15\rho_{\text{nuc}}$. The equation of state is unknown. It could consist of quark matter, hyperons (baryons that contain strange quarks), pions, or kaons... we don't really know.

### 4.3 Superfluidity

At temperatures less than some critical temperature $T_c$, we get superfluidity, which is a phenomenon that does not affect the equation of state. It does, however, affect heat capacity and thus neutron star cooling. Protons become superconducting and the magnetic field becomes quantized into flux tubes. The magnetic field freezes in the crust, causing co-rotation of the crust and core (making essentially solid-body rotation).

## 5 X-Ray Binaries

An **X-Ray Binary** (XRB) is a binary consisting of a neutron star or black hole with some other companion. Their radiation peaks at $0.1 - 100$ keV. The radiative efficiencies of their accretion power are

$$\eta_{\text{NS}} = \frac{GM}{Rc^2} \approx 0.1 \tag{5.1}$$

for a neutron star and about 0.4 for a black hole. This means that 10 and 40 percent of the rest energy of accreted material is radiated away upon accretion. This means that the energy generation rate per unit mass is approxmately

$$\epsilon_{\text{NS}} \sim 10^{20} \text{ erg g}^{-1} \tag{5.2}$$

Compare this to hydrogen fusion, which has only $\epsilon_{\text{CNO}} = 6 \times 10^{18}$ erg g$^{-1}$ $\approx 0.007c^2$. The luminosity of X-Ray binaries is usually Eddington-limited, with $L = L_{\text{Edd}} \sim 10^{38}$ erg s$^{-1}$ and an accretion rate of $\dot{M} \sim 10^{-8}\ M_\odot$ yr$^{-1}$. Comparing this luminosity to a typical radius of $R \sim 10^6$ cm gives a blackbody temperature of $T \approx \times 10^7$ K. So, these are *hot* surfaces. This corresponds to a frequency of $\nu = 1.2 \times 10^{18}$ Hz, a wavelength of $\lambda = 25$ Å, or a photon energy of $h\nu = 5$ keV.

We encounter XRBs in two main flavors. The first is a **Low Mass X-Ray Binary** (LMXRB), which consists of a neutron star and a main sequence star that is undergoing Roche lobe overflow onto its compact companion. A prime example of a LMXRB is the 1972 discovery of Her X-1 with its 1.24 second period (which is the rotation period of the neutron star) and a secondary 1.7 day period (which is the period of the orbit). Additionally, we observe **High Mass X-Ray Binaries** (HMXRB), which have a neutron star and an OBstar that is emitting matter via a wind, such as Cen X-3 (1971), which has a 2.1 day period.

The maximum temperature will occur when free falling matter hits the neutron star surface at $v_{\text{ff}} \sim 0.1c$. This gives a temperature of

$$\frac{1}{2} m_p v_{\text{ff}}^2 = \frac{3}{2} k T_{\text{eff}} \qquad \Rightarrow \qquad T_{\text{eff}} = 3.6 \times 10^{12} \left( \frac{v_{\text{ff}}}{c} \right) \text{ K} \tag{5.3}$$

Where the free fall velocity is

$$v_{\text{ff}} = \left( \frac{2GM}{r} \right)^{1/2} \tag{5.4}$$

Usually we see $T \sim T_{\text{Blackbody}}$ rather than $T_{\text{ff}}$.

## 5.1 Magnetic Inflows

The intense magnetization of neutron stars (e.g. $B \sim 10^{12}$ G) can also disrupt the usual accretion flow at the magnetic (or Alfvén) radius, $R_{\rm M}$, at which the magnetic field pressure equals the ram pressure of freefall. Algebraic, this condition is denoted by

$$\rho v_{\rm ff}^2 = \frac{B^2}{8\pi} \tag{5.5}$$

where $B^2$ has energies of energy per volume (i.e., pressure). If we have spherical symmetry, the accretion rate is

$$\dot{M} = 4\pi r^2 \rho v_{\rm ff} \tag{5.6}$$

and the magnetic field is

$$|B| = \frac{\mu}{r^3} \sim 10^{12} \text{ G} \quad \text{where } r = R_{\rm NS} \tag{5.7}$$

where $\mu$ is the magnetic dipole moment of the neutron star. We can solve eq. (5.6) for the density at $r = R_{\rm M}$ to get

$$\rho = \frac{\dot{M}}{4\pi R_{\rm M} v_{\rm ff}} \tag{5.8}$$

where now

$$v_{\rm ff} = \left(\frac{2GM}{R_{\rm M}}\right)^{1/2} \tag{5.9}$$

Then the condition to find $R_{\rm M}$, eq. (5.5), becomes

$$\frac{(2GM)^{1/2}\dot{M}}{4\pi R_{\rm M}^{5/2}} = \frac{\mu^2}{8\pi R_{\rm M}^6} \tag{5.10}$$

Solving this for $R_{\rm M}$ gives us

$$R_{\rm M} = (8G)^{-1/7}\mu^{4/7}\dot{M}^{-2/7}M^{-1/7} \tag{5.11}$$

Now if we use the XRB's luminosity as $L_X = GM\dot{M}/R$ to parameterize $R$, we get

$$R_{\rm M} = 2.9 \times 10^8 \text{ cm} \left(\frac{M}{M_\odot}\right)^{-1/7} \left(\frac{R}{10^6 \text{ cm}}\right)^{-2/7} \left(\frac{L_X}{10^{37} \text{ erg s}^{-1}}\right)^{-2/7} \times \left(\frac{\mu}{10^{30} \text{ G cm}^{-3}}\right)^{4/7} \approx 3 \times 10^8 \text{ cm} \tag{5.12}$$

This radius is several hundred neutron star radii, so this magnetic distortion is an observable effect. The picture is then some accretion disk that has some inner radius where matter is then channeled along field lines to the polar caps. Such a configuration is shown in Figure 5. The magnetic channeling of material causes a relatively small magnetic cap area to be heated by the infalling plasma. The incoming matter int his region will be revolving about the magnetic fields at the cyclotron frequency, which for electrons is

$$E_{\rm cyc} = h\nu_e = 11.6 \left(\frac{B}{10^{12} \text{ G}}\right) \text{ keV} \tag{5.13}$$

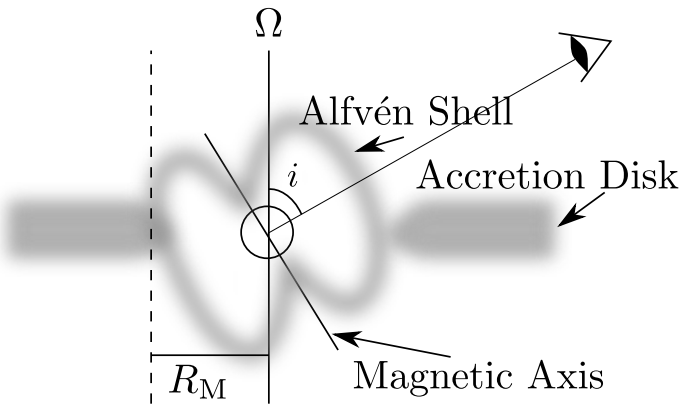


Figure 5: A sketch of magnetically distorted accretion. Material outside $R_{\rm M}$ forms a normal accretion disk, but within $R_{\rm M}$, it is channeled along magnetic field lines to the magnetic polar caps, which may or may not be along the same axis as the rotation axis.

and for protons

$$E_{\rm cyc} = h\nu_p = 6.3 \left( \frac{B}{10^{15}\ {\rm G}} \right)\ {\rm keV} \tag{5.14}$$

So the energies of these particles are quantized for motion perpendicular to the field. These quantized levels are called Landau levels and are given by

$$h\nu = (n + \frac{1}{2} + s)E_{\rm cyc} \tag{5.15}$$

where $n$ is the quantum number and $s = \pm 1/2$ is the spin of the particle. Thus there will be increased Compton scattering at these quantized energies, which was seen in M Her X-1 in the 1970s in the absorption spectrum. The relativistic redshift is important here, too, since $h\nu_{\rm obs} = h\nu_{\rm cyc}/(1+z)$.

We already stated that the magnetic field may be misaligned with the rotation axis. This misalignment gives rise to X-Ray pulsations. These, too, are observed. For example, a period of 0.7145 s is observed in SMC X-1 and 0.069 in A05388-66 (cool name, huh?).

The accreted material can also act to spin up the neutron star by taking angular momentum from the disk and depositing it in the neutron star. For example, millisecond pulsars are found in binaries and are thought to have been spun-up over the course of their accretion lives.

## 5.2 Pulsar Spindown

If a relatively slowly spinning neutron star can be spun up by accreting material, a rapidly-rotating neutron star should be able to spun *down* by the accreted material. For example, the Crab pulsar, which is a remnant of SN 1054 has a period of $P = 33$ ms, but it is slowing down at $dP/dt \sim 1$ ms/(100 yrs).

If we approximate a neutron star as a uniform sphere, then the moment of inertia is

$$I = \frac{2}{5}MR^2 = 2.5 \times 10^{45} \left(\frac{M}{1.4\ M_\odot}\right)\left(\frac{R}{1.5 \times 10^6\ \text{cm}}\right)^2\ \text{g cm}^2 \tag{5.16}$$

The crab pulsar spins down at a rate

$$\frac{d\omega}{dt} = -2.4 \times 10^{-9}\ \text{s}^{-2} \tag{5.17}$$

where $\omega$ is the angular velocity. This implies a spin-energy loss rate (using $E_{\text{rot}} = \frac{1}{2}I\omega^2$) of

$$\frac{dE_{\text{rot}}}{dt} = I\omega\frac{d\omega}{dt} \approx 4.6 \times 10^{38}\ \text{erg s}^{-1} \tag{5.18}$$

This is comparable to the crab nebula luminosity of $5 \times 10^{38}$ erg/s. That is, the energy that is being radiated could very well be taken from the rotational velocity. To model this, we'll use the so-called oblique rotator model, where the magnetic dipole and rotation axes are misaligned by some angle $\alpha$. An observer at infinity will just see a changing magnetic dipole moment, which we will designate as $\mathbf{m}$. This is given in terms of the magnetic field and radius as

$$|\mathbf{m}| = \frac{B_p R^3}{2} \tag{5.19}$$

where $B_p$ is the magnetic field at the pole of the neutron star and $R$ is the radius of the star. Using this language, the energy loss rate would be

$$\left(\frac{dE}{dt}\right)_{\text{WD}} = -\frac{2}{3c^3}m^2\omega^4\sin^2\alpha \tag{5.20}$$

for the crab pulsar, we have $m \sin\alpha \sim 4 \times 10^{30}$ G cm$^3$ and an implied magnetic field of $B \sim 10^{12}$ G. We can rewrite the energy loss as

$$\dot{E} = -\frac{2}{3c^3}\left|\ddot{\mathbf{m}}\right|^2 = -6.2 \times 10^{27}\ \text{erg s}^{-1} \left(\frac{B_p}{10^{12}\ \text{G}}\right)^2\left(\frac{R}{10^6\ \text{cm}}\right)^6\left(\frac{\omega}{1\ \text{s}^{-1}}\right)^4\sin^2\alpha \tag{5.21}$$

Now if we set $\dot{E}_{\text{MD}} = \dot{E}_{\text{rot}}$, we get the spindown rate:

$$\dot{\omega} = -\frac{B_p^2 R^6 \omega^3 \sin^2\alpha}{6c^3 I} \tag{5.22}$$

The negative sign means that the spin must slow down. We've also been assuming $B$ is not changing. For reference, this gives the crab nebula a period of $P = 0.033$ s and a spindown rate of $\dot{P} = 4.2 \times 10^{-13}$ s s$^{-1}$. Now since $\dot{\omega} = -C\omega^3$ for some constant $C$, we get

$$\int_{\omega_0}^{\omega}\frac{d\omega}{\omega^3} = -\int_0^t c\,dt \tag{5.23}$$

Simplifying this, we get

$$\frac{1}{2C}\left[\frac{1}{\omega^2} - \frac{1}{\omega_0^2}\right] = t > \frac{1}{2C\omega^2} \tag{5.24}$$

For the crab, this max value is 1247 years (not bad!), so it appears that dipole braking is a good understanding of what's going on. Note that since at early times, spindown occurs much more rapidly, a good measurement of $\omega_0$ is not really necessary for a good measurement. We can also define a dipole timescale:

$$\tau_{\text{dipole}} = -\left(\frac{\omega}{2\dot{\omega}}\right) = \left(\frac{P}{2\dot{P}}\right) \tag{5.25}$$

which is the timescale on which the period is changing significantly.

Note that using $\dot{E}$ for the crab pulsar, the magnetic dipole model and $\sin\alpha = 1$ gives a polar magnetic field of $B_p = 5.2 \times 10^{12}$ G. One might wonder where such strong magnetic fields come from. On a typical MS star, there is typically a $\approx 100$ G magnetic field at the surface. A decrease in the radius by a factor of $10^5$ causes an increase in $B_p$ of $10^{10}$. So long as magnetic flux is conserved, such compact objects should always have very strong magnetic fields.

**Braking Index** For any power-law deceleration model (like the magnetic dipole model we've presented), we can write $\dot{\omega} = -(\text{constant})\omega^n$, where $n$ is called the **braking index**. So as we've seen, $n = 3$ for the magnetic dipole model. In general, we have

$$n \equiv -\frac{\omega\ddot{\omega}}{\dot{\omega}^2} \tag{5.26}$$

Another important case is that of gravitational wave radiation, where $n = 5$. The more general pulsar age formula is then

$$t = -\frac{1}{n-1}\left(\frac{\omega}{\dot{\omega}}\right)\left[1 - \left(\frac{\omega}{\omega_0}\right)^{n-1}\right] \tag{5.27}$$

And so the characteristic age (assuming $\omega \ll \omega_0$) is

$$\tau = -\frac{1}{n-1}\left(\frac{\omega}{\dot{\omega}}\right) \tag{5.28}$$

Doing this calculation, the crab pulsar gives $n = 2.515$ and from PSR 1507-58, we get $n = 2.83$. So it seems that magnetic dipole braking is not the whole story.

## 5.3 Pulsar Characteristics

*Monday, May 6, 2013*

There are two main classes of pulsars. The first are what we've been talking about, the rotationally powered (radio) pulsars that were first detected back in the 1940's. Additionally, there are accretion-powered (or x-ray) pulsars. Both convert spin energy into radiation, and the energy they radiate in various wavelengths varies dramatically. Table 5.3 demonstrates that only a small fraction of the total energy available due to spindown is emitted as photons. It is thought that a lot of the remaining energy goes in to driving powerful winds (outflows), making a pulsar wind nebula. Such objects are called **plerions**. The spectra of such objects can have a thermal component and a power law component around a keV. The thermal portion comes from the neutron star surface, and the power law comes from the acceleration of charged particles in the outflow.

| wavelength | $\dot{E}/\dot{E}_{\rm dip}$ |
|---|---|
| radio | $10^{-7}$ |
| optical | $10^{-5}$ |
| X-ray | $10^{-4} - 10^{-3}$ |
| $\gamma$-ray | $10^{-2} - 10^{-1}$ |

Table 4: relative energy distributions as a fraction of the spindown power.

There are several proposed mechanisms for how a pulsar emits the radiation that we observe. The first is the simple case of an aligned magnetic field and rotation axis. We assume a perfectly conducting sphere, in which case the electrons rearrange themselves to remove the magnetic fields. A dipole magnetic field scales as

$$\mathbf{B} = B_P R^3 \left( \frac{\cos\theta}{r^3}\hat{r} + \frac{\sin\theta}{2r^3}\hat{\theta} \right) \tag{5.29}$$

The rearrangement of the charges gives rise to an electric field following

$$\mathbf{E} + \left( \frac{\mathbf{\Omega} \times \mathbf{r}}{c} \right) \times \mathbf{B} = 0 \tag{5.30}$$

Near the pole, then, this is

$$E_p \approx \frac{R\Omega B_P}{c} \approx 6 \times 10^{16} \left( \frac{P}{1 \text{ sec}} \right)^{-1} \left( \frac{B_P}{10^{12} \text{ G}} \right) \text{ V cm}^{-1} \tag{5.31}$$

Such electromagnetic fields have a powerful effect on charged particles following the Lorentz force law:

$$\mathbf{F} = \frac{q}{c}\mathbf{v} \times \mathbf{B} \tag{5.32}$$

For protons, this gives a force (relative to the gravitational force) of

$$\text{protons}: \frac{F_{\rm EM}}{F_{\rm G}} \sim \frac{qR\Omega B_p/c}{GMm_p/R^2} \sim 10^9 \gg 1 \tag{5.33}$$

and approximately $10^{11}$ for electrons. As a result, electrons are simply ripped from the neutron star's surface by this intense Lorentz force, tied to magnetic field lines. The magnetic field and plasma then co-rotate with the neutron star uot to the light cylinder of $R_c \equiv c/\Omega = 5.9 \times 10^{11}$ cm$(P/1$ sec$)$. Past that point there is little or no rotation of the magnetic field lines. Thus, field lines that remain in the light cylinder can stay "closed", but those that pass outside the light cylinder will necessarily not closed, and the field lines wind up as the pulsar spins. These free lines can carry matter out of the system, but the exact mechanism isn't well understood. Some models assocate pulses with the polar caps, while others do so with the so-called gap regions, which are the regions in between the open and closed magnetic field lines.

It's believed that electrons can produce **curvature radiation**, which is similar to synchrotron radiation, but not the same. As they spin around the field lines, they emit synchrotron radiation, but as the velocity perpendicular to the field line vanishes, they shoot out *along* the *curved* field line.

Thus it is like synchrotron radiation, but with the radius set by the curvature of the magnetic fields along which they travel. ??? brings the temperature so high in the neutron star that the it radiates emission that must be coherent. Particles radiating in bunches coherently, not synchrotron. This causes gamma rays, which induces pair-production, which then interacts with the magnetic field, which causes more gamma rays. This is not really well understood, and has admittedly been copied to these notes in low fidelity. Sorry.

So far we've focused on spindown-powered pulsars. Now we focus our attention on accretion-powered pulsars. These have spin periods ranging from 7.5 ms to 3 hours, though most are in the range of 1-1000 seconds. Most are HMXRBs, containing O and B star companions (and accretion through polar caps), though some are indeed LMXRBs. Before delving too deep into the general field of accretion-powered pulsars, we should take a brief detour into magnetars.

**Magnetars** Typical neutron stars have magnetic fields of $B \sim 10^{12}$ G. Some, though, have them as large as $B \sim 10^{14} - 10^{16}$ G. These are the so-called magnetars. If the magnetic field is strong enough, the Larmour radius of electrons becomes smaller than the de Broglie wavelength:

$$r_{\rm L} = \frac{vM_e c}{eB} \qquad \lambda = \frac{h}{m_e v} \tag{5.34}$$

In situations such as this, there is a quantum critical field, above which quantum mechanics becomes important for electrons in the process. Just setting these two lengthscales together, we get a magnetic field of

$$B_{\rm QC} = \frac{m_e^2 c^3}{he} = 4.4 \times 10^{13} \text{ G} \tag{5.35}$$

**Anomalous X-Ray Pulsars** These AXPs are isolated pulsare that emit pulsed -rays with luminosities on the order of $L \sim 10^{35-36}$ erg s$^{-1}$ and periods of $P \sim 5 - 12$ s. Such a luminosity is too high for magnetic dipole radiation, so it is assumed (read: guessed) that is is from a dissipation of a strong magnetic field. The characteristic spin-down timescale of 3-100 kyr. These are not typical radio pulsars, with magnetic fields with strengths of $B \sim 10^{14} - 10^{16}$ G, so these are more like magnetars.

**Soft Gamma-Ray Repeaters** Soft Gamma-Ray Repeaters, or SGRs, are essentially $\gamma$-ray lighthouses with a thermal spectrum peaking at a few keV. They have periods of $5 - 8$ s with spindown rates of $\dot{P} \approx 7 \times 10{-}4$. Their high magnetic fields put them in the magnetar category, and they are thought to be a young supernova remnant. They are capable of dramatic flares. For instance, one flare, lasting from 1806-1820 gave off approximately $E \sim 2 \times 10^{46}$ erg under a magnetic field of $B \sim 1.6 \times 10^{15}$ G. The energy contained in the magnetic field is then

$$E_{\rm mag} \sim \frac{B^2}{8\pi} \frac{4\pi}{3} R^3 \sim 10^{48} \text{ erg} \tag{5.36}$$

so the flares give off about 1% of the magnetic energy in their blast. They are thought to be the result of a stellar "quake" that rearranges the magnetic field.

**MilisecondPulsars / Recycled Pulsars** Millisecond pulsars (pulsars that have periods on the order of 1 ms), or recycled pulsars, as they are sometimes referred, often occur (75% of the time) in binaries. As a result, we understand their short periods to be a result of angular momentum transfer from a companion through RLOF, giving them an unusually short period. They have small period derivatives and long spin-down ages in of $10^9 - 10^{10}$ yrs. They *should* have shut off, but due to the spin-up from their companion, they have been "recycled". Those without companions are thought to have evaporated or tidally disrupted their donors.

**X-Ray Pulsars** These are accretion-powered (rather than spindown-powered) pulsars with spin periods of 2.5ms - 3 hours (with most between 1 and 1000 seconds). Most are in HMXB configurations with an O- or B- type star companion. They generate X-Rays, likely through polar cap accretion. Rotation still should provide the pulsing nature of these objects

**Pulsar Glitches** Some pulsars will have their spin velocity speed up suddenly. The cause is unkown, but thought to be quakes and/or cracks in the crystalline crust. These cause the moment of inertia to decrease, resulting in a increase in angular velocity. For example, the Vela pulsar has had a glitch with $\Delta\Omega/\Omega \sim 10^{-2}$. More characteristically, we've observed glitches with $\Delta\Omega/\Omega \sim 10^{-6}$.

**Neutron Star Cooling** Neutron stars are born with very high temperatures ($T \sim 10^{11}$ K) from a supernova. They radiate $10^{53}$ erg in their first few seconds, and after a day, the temperature has dropped around an order of magnitude to $T \sim 10^{10}$ K. For the first $\sim 10^5$ years, neutrino emission dominates the heat loss down to $T \sim 10^6$ K. Below this temperature, photon radiation from the surface takes over. The surface temperatures are still quite high at $T_{\rm surf} \sim 5 \times 10^5$ K, giving a thermal emission strong in the UV/soft X-ray.

# 6 Accretion Disks

*Wednesday, May 8, 2013* To begin talking about accretion disks, we need to first set upa coordinate system. We'll assume cylindrical symmetry where $r$ is the radial coordinate and $\phi$ is the azimuthal angle, and $z$ is the height coordinate along the symmetry axis. Then for a Keplerian disk, the azimuthal velocity is

$$v_\phi = \Omega r = \left(\frac{GM}{r^3}\right)^{1/2} r = \left(\frac{GM}{r}\right)^{1/2} \propto r^{1/2}. \tag{6.1}$$

Again, this result only applies if matter is falling in roughly cirecular, Keplerian orbits. Thus, different annuli rotate at different speeds, decreasing with increasing radial distance. Though the azimuthal velocity decreases with $r$, the specific angular momentum (angular momentum per unit mass) *increases* with $r$ as

$$\ell = v_\phi r = (GMr)^{1/2} \propto r^{1/2} \tag{6.2}$$

So $\ell$ is larger at larger radii and $v$ is smaller. Thus, for a ring of gas to fall in, it must lose $\ell$ and since $\ell_{\rm tot}$ is conserved, angular momentum must flow out of the disk. That is to say, angular momentum is concentrated in the outer "rings" in order to allow the inflow of matter to tighter orbits.

The viscosity between parcels couples the angular momentum transport. Consider two rings of material orbiting at Keplerian orbits. The outer ring, rotating more slowly, *drage* the inner ring,

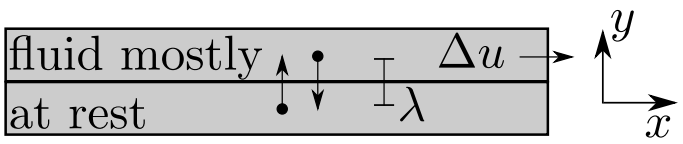


Figure 6: Schematic of a disk layer where viscous transfer is occurring.

decelerating it, causing it to fall inward. This, in turn, accelerates material in the outer ring and drives it to larger $r$ and larger $\ell$. The net effect is that

> Angular momentum is transported outward while mass is transported inward, causing the gas to be heated through friction. This heat is loss in situ.

The Virial Theorem tells us that half the binding energy released upon reaching a distance $r$ can be dissipated as local heat. Then the luminosity of the disk is

$$L_{\rm disk} = \frac{GM_1\dot{M}}{2R_{\rm in}} = \frac{1}{2}L_{\rm acc} \tag{6.3}$$

where $L_{\rm acc} = GM_1\dot{M}/R_{\rm in}$, $M_1$ is the mass of the accreting star, and $R_{\rm in}$ is the inner radius of the accretion disk. Viscosity is essential for this process. Consider two adjacent fluid layers with a velocity drift (relative difference in azimuthal velocity) $\Delta u$, depicted in Molecules will move back and forth between the parcels with velocity $v_y$, transporting the $x$-component of the fluid momentum. This occurs over some lengthscale $\lambda$ depending on $v = v_y$. This is quantified by **kinematic viscocity**, defining the viscosity to be $\nu \sim \lambda v_y$, which naturally has the units of specific angular momentum. $\lambda$ is the molecular mean free path and $v \sim c_s$ is roughly the sound speed.

It's convenient to quantify the turbulence via the **Reynolds Number**,

$$R_e \equiv \frac{Rv_y}{\nu} \tag{6.4}$$

($R$ is some characteristic lengthscale). This is the ratio of inertial forces to viscous forces, where $\nu$ is the molecular viscosity. If we plug in actual numbers, we get huge Reynolds number ($> 10^{12}$), implying very strong turbulence. Then instead of using the sound speed, the appropriate viscosity might be

$$\nu_{\rm turb} \sim \lambda_{\rm turb} v_{\rm turb} \tag{6.5}$$

where $\lambda_{\rm turb}$ is the eddy lengthscale and $v_{\rm turb}$ is the eddy velocity. If we assume the height of a turbulent eddy is $H$ at any $r$, then the lengthscale is $\lambda_{\rm turb} \lesssim H$ and $v_{\rm turb} \lesssim c_s$:

$$\nu = \alpha c_s H \tag{6.6}$$

This is the Shakura & Sunyaev (1973) "solution", which parameterizes all unknowns into $\alpha$, which is typically in the range of $10^{-3}$ to 1, as determined observationally. Such "$\alpha$-disks" must be "thin". Now we'll figure out the conditions under which this works well.

## 6.1 Conditions for a Thin Accretion Disk

Supposing that hydrostatic equilibrium support is in the $z-$direction (perpendicular to the plane). HSE tells us

$$\frac{\partial P}{\partial z} = -\frac{GM\rho \sin\theta}{r^2} \tag{6.7}$$

This is the fraction of the pressure support that supports the material above the *disk*, not from the gravitational source. We can approximate the angular dependence using the small angle approximation as

$$\sin\theta \sim \frac{z}{r} \sim \frac{H}{r} \qquad \Rightarrow \qquad \mathcal{O}\left(\frac{dP}{dr}\right) \sim \frac{P}{H} \tag{6.8}$$

giving us

$$\frac{P}{H} \approx \frac{GM\rho z}{r^3} \tag{6.9}$$

Now if the gas is Keplerian, then we have the usual azimuthal velocity, $v_\phi^2 = GM/r$ and so we can use this in our HSE calculation:

$$\frac{P}{H} \approx v_\phi^2 \frac{1}{r^2}\rho H \tag{6.10}$$

$$\frac{P}{\rho} \approx \frac{v_\phi^2}{r^2} H^2 \sim c_s^2 \tag{6.11}$$

$$\frac{H}{r} \approx \frac{c_s}{v_\phi} \sim \frac{1}{\text{mach }\#} \tag{6.12}$$

For $H/r \ll 1$, then $c_s \ll v_\phi$, meaning that rotation velocities are much larger than the internal velocities. Thus the internal pressure gradient doesn't inflate the disk. Instead, they are Keplerian with $H/R \lesssim 0.01$.

Now we'd like to understand what the luminosity from such a disk would be in a steady state configuration. We'll integrate the energy dissipation rate as a function of radius, defining a flux density

$$\epsilon = \frac{\text{Energy}}{\text{Area} \times \text{time}} = \left[\frac{g}{\text{sec}^3}\right] \tag{6.13}$$

And so the luminosity would be

$$L = \int_R \epsilon A \tag{6.14}$$

We'll need to use three things to quantify this result

1. Torques: these manifest a different angular velocity versus radius relation $d\Omega/dr$
2. Viscosity ($\nu$)
3. Surface density ($\Sigma$)

The energy flux is just

$$\epsilon = \nu\Sigma \left(\frac{d\Omega}{dr}\right)^2 r^2 \tag{6.15}$$

We'll need to know a bit more about the structure of accretion disks in order to dig deeper, into the $\nu\Sigma$ terms, but we'll assume Keplerian flows for $d\Omega/dr$.

## 6.2 Structure of Accretion Disks

For a steady-state disk, the inflow velocity $v_r$ is determined by $\nu$. Conservation of mass implies that the steady-state mass flow through any radius is constant. The accretion rate can be written as

$$\dot{M} = 2\pi r v_r \int \rho(r,z)\, dz = \text{const} = 2\pi r v_r \Sigma(r) \tag{6.16}$$

where we have used $\Sigma(r) = \int \rho(r,z)\, dz \sim \rho H$. This will come in handy momentarily, but now we calculate the viscous torque acting on a cylindrical surface at radius $r$:

$$G(r) = 2\pi r^3 \nu \Sigma \frac{d\Omega}{dr} \tag{6.17}$$

so the net torque in a small region $\delta r$ at $r$ is just the difference between those two locations:

$$\Delta G = G(r) - G(r+\delta r) = \frac{\partial G}{\partial r}\delta r \tag{6.18}$$

Such viscous torques must be related to the change of the angular momentum at the a distance $r$:

$$G(r) = \frac{dL}{dt} = \frac{d}{dt}(m v_\phi r) = \dot{M} v_\phi r \tag{6.19}$$

$$= 2\pi r^2 v_\phi v_r \Sigma(r) \tag{6.20}$$

$$= 2\pi r^3 \Omega v_r \Sigma(r) \tag{6.21}$$

where we've made use of eq. (6.16) to eliminate the accretion rate. Differentiating this result, we get

$$\frac{dG}{dr} = 2\pi \frac{d}{dr}\left(r^3 \Sigma v_r \Omega\right) \tag{6.22}$$

Integrating this result and equating it to what we found in eq. (6.17), we get

$$G = 2\pi r^3 \Sigma v_r \Omega + C \tag{6.23}$$

$$2\pi r^3 \nu \Sigma \frac{d\Omega}{dr} = 2\pi r^3 \Sigma v_r \Omega + C \tag{6.24}$$

$$\nu \Sigma \frac{d\Omega}{dr} = \Sigma v_r \Omega + \frac{C}{2\pi r^3} \tag{6.25}$$

$C$ is related to the boundary condition imposed on the orbit (see Longair or Frank, King, and Raine). It ends up being

$$C = -\dot{M}(G_{\text{grav}} M_* r_*)^{1/2} \tag{6.26}$$

where the quantity in parentheses is $\ell$ at the last (innermost) orbit. If we substitute in for $C$, $\dot{M}$, and suppose $\Omega = \Omega_{\text{K}}$ (the Keplerian result), we get

$$\boxed{\nu\Sigma = \frac{\dot{M}}{3\pi}\left[1 - \left(\frac{r_*}{r}\right)^{1/2}\right]} \tag{6.27}$$

So now that we have $\nu\Sigma$, we can get back to the energy dissipation per unit area, $\epsilon$. If we assume Keplerian orbits again, we know $d\Omega/dr$, so then

$$\epsilon = \nu\Sigma r^2 \left(\frac{d\Omega}{dr}\right)^2 \tag{6.28}$$

$$= \frac{9}{8}\nu\Sigma\frac{GM_*}{r^3} \tag{6.29}$$

$$= \frac{3G\dot{M}M_*}{4\pi r^3}\left[1-\left(\frac{r_*}{r}\right)^{1/2}\right] \tag{6.30}$$

Now we can integrate this to get the luminosity of the disk again

$$L = \int_{r_*}^{\infty} \epsilon 2\pi r\, dr = \frac{G\dot{M}M_*}{2r_*} \tag{6.31}$$

which is pretty much exactly what we said earlier as a result of the Virial theorem. Now if we use the Stefan-Boltzmann law, we can get a temperature profile since $\sigma T^4 = \epsilon$ (remember that $\epsilon$ is essentially a radiative flux). This gives a temperature profile of

$$T(r) = \frac{3GM_*\dot{M}}{8\pi r^3\sigma}\left[1-\left(\frac{r_*}{r}\right)^{1/2}\right]^{1/4} \tag{6.32}$$

So for $r \gg r_*$, the limiting result is

$$T = T_*\left(\frac{r}{r_*}\right)^{-3/4} \tag{6.33}$$

where for a white dwarf, we typically find $T_* \sim 4\times10^4$ K and for neutron stars, $T_* \sim 10^7$ K. Note that it is likely wiser to refer to $r_*$ as $r_{\rm inner}$, since this is also true for black holes. This changes the boundary condition for $C$ to

$$C \to \beta\dot{M}\left(GMr_{\rm inner}\right)^{1/2} \tag{6.34}$$

with $R_{\rm inner} = 6GM/c^2$ for a Schwarzschild black hole.

*Monday, May 13, 2013*
Earlier we found that the temperature in the accretion disk varies as

$$T_{\rm eff} \propto R^{-3/4} \tag{6.35}$$

At each radius, the intensity of radiation is given by the Planck function

$$I_\nu(R) = B_\nu[T(R)]; \qquad B_\nu = \frac{2h\nu^3}{c^2}\frac{1}{e^{h\nu/(kT(R))}-1} \tag{6.36}$$

If an observer is at a distance $D$ with a line of site making an inclination angle $i$, the observed flux is

$$F_\nu = \int_{r_*}^{r_{\rm out}} I_\nu\, d\Omega(R) \tag{6.37}$$

where

$$d\Omega(R) = \frac{2\pi r\, dr\, d\phi}{D^2} \tag{6.38}$$

is the solid angle subtended by an infinitesimal part of the accretion disk. Expanding this out, we get

$$F_\nu = \frac{4\pi h\nu^3 \cos i}{c^2 D^2} \int_{r_*}^{r_{\rm out}} \frac{r\,dr}{\exp\left(\frac{h\nu}{kT(R)}\right) - 1} \tag{6.39}$$

In the Raleigh-Jeans limit of low photon energies, this reduces to (assuming $\nu \ll kT(R_{\rm out})/h$) a flux scaling as

$$B_\nu \approx \frac{2kT(R)\nu^2}{c^2} \qquad \Rightarrow \qquad F_\nu^{\rm RJ} \propto \nu^2 \tag{6.40}$$

In the high energy limit, $\nu \gg kT(R_*)/h$, we get the Wien result:

$$B_\nu^W \approx \frac{2h\nu^3}{c^2} e^{-\frac{h\nu}{kT}} \tag{6.41}$$

and the flux density in the inner, hotter regions is given by

$$F_\nu^W \propto \nu^3 e^{-h\nu/kT} \tag{6.42}$$

In between these two regimes we need to consider the true sum of the blackbodies. We change variables to

$$\eta \equiv \frac{h\nu}{kT(R)} \approx \frac{h\nu}{kT(R_*)} \left(\frac{R}{R_*}\right)^{-3/4} \tag{6.43}$$

So the observed flux is now, in terms of $\eta$,

$$F_\nu \propto \nu^{1/3} \int_0^\infty \frac{\eta^{5/3}}{\exp(\eta) - 1} d\eta \tag{6.44}$$

So then $F \propto \nu^{1/3}$ in intermediate regions. The resulting spectrum has three regions. With the low- and high-energy regions scaling accordingly, connected by this $nu^{1/3}$ region.

## 6.3 Full Shakura/Sunyaev Solution

$$f = \left[1 - \left(\frac{R_*}{R}\right)^{1/2}\right]^{1/4} \tag{6.45}$$

For convenience, we'll make the following definitions

$$R_{10} = \frac{R}{10^{10}\ {\rm cm}} \qquad \dot{M}_{16} = \frac{\dot{M}}{10^{16}\ {\rm g\ s^{-1}}} \qquad M = \frac{M_*}{M_\odot}. \tag{6.46}$$

Then the surface density is

$$\Sigma = 5.2\alpha^{-4/5} \dot{M}_{16}^{7/10} M^{1/4} R_{10}^{-3/4} f^{14/5}\ {\rm g\ cm^{-2}}, \tag{6.47}$$

and the height of the disk is

$$H = 1.7 \times 10^8\ {\rm cm}\ \alpha^{-1/10} \dot{M}_{16}^{3/20} M^{-3/7} R_{10}^{-9/5} f^{3/5}. \tag{6.48}$$

The density is

$$\rho = 3.1 \times 10^{-5} \text{ g cm}^{-3} \alpha^{-7/10} \dot{M}_{16}^{11/20} M^{5/8} R_{10}^{-15/8} f^{11/5}. \tag{6.49}$$

The central temperature is given by

$$T_c = 1.4 \times 10^4 \text{ K } \alpha^{-1/5} \dot{M}_{16}^{3/10} M^{1/4} R_{10}^{-3/4} f^{6/5}. \tag{6.50}$$

The optical depth is

$$\tau = 1.9 \ \alpha^{-4/5} \dot{M}^{1/5} f^{4/5} \tag{6.51}$$

The viscosity is

$$\nu = 1.8 \times 10^{14} \text{ cm}^2 \text{ s}^{-1} \ \alpha^{4/5} \dot{M}_{16}^{3/(r)?} M^{-1/4} R_{10}^{-1/4} f^{-14/5}. \tag{6.52}$$

The radial and azimuthal velocities are given by

$$v_R \sim 0.3 \text{ km s}^{-1} \qquad \text{and} \qquad v_\phi \sim 1000 \text{ km s}^{-1} \tag{6.53}$$

So the rotational velocity is supersonic, but the rotational drift velocity is subsonic.

## 6.4 A Few More Tidbits

Note that the height is an increasing function of $r$:

$$\frac{dH}{dr} \propto r^{1/8} \tag{6.54}$$

so accretion disks are flared towards their outsides.

Secondly, our assumptions may be inconsistent with the solution. The critical accretion rate is of course the Eddington limit:

$$\dot{M}_{\text{crit}} = \frac{L_{\text{Edd}} R_*}{2\eta G M} = 1.5 \times 10^{18} \left( \frac{R_*}{3 \text{ km}} \right) \left( \frac{\eta}{0.1} \right)^{-1} \text{ g s}^{-1} \tag{6.55}$$

where $\eta$ is the radiative efficiency of the flow. The ratio of the height to the radius, though, is

$$\frac{H}{R} \sim \frac{3}{4\eta} \frac{\dot{M}}{\dot{M}_{\text{crit}}} \left[ 1 - \left( \frac{R_*}{R} \right)^{1/2} \right] \tag{6.56}$$

So as $\dot{M} \to \dot{M}_{\text{crit}}$, $H/R \geq 1$ near $R = 2R_*$. At this point, radiation pressure is greater than the thermal pressure.

Thirdly, we must consider thermal stability. If $T_c \gtrsim 10^4$ K and the disk is optically thin, the cool areas cool more rapidly, leading to large temperature fluctuations, causing the solution to be unstable.

Finally, we should consider viscous stability. A steady-state flow is stable only if

$$\left( \frac{\partial(\nu\Sigma)}{\partial\Sigma} \right) > 0 \tag{6.57}$$

otherwise the disk becomes unstable.

## 6.5 More General Flows

The standard Shakura/Sunyaev Solution thus far has assumed

1. Viscous energy is radiated where it was produced in the disk
2. Gas pressure provides the support
3. Motion is purely toroidal

We should consider a more general situation where **advection** is allowed. Advection it hte transport of energy and mass in bulk by large-scale motions in a fluid, whereas convection is flow when diffusive and advective motions are important.

Now if the fluid can carry thermal energy inward (advect it), then the heating per unit volume can be modeled via

$$q_{\rm adv} = \underbrace{q_+}_{???} - \underbrace{q_-}_{\text{radiative cooling}} \tag{6.58}$$

There are three limiting cases here:

1. $q_{\rm adv} \ll q_+ - q_-$ (SS disk)
2. $q_- \ll q_{\rm adv} \sim q_+$ Advection-dominated accretion flow(ADAF)
3. $q_+ - q_- \approx -q_{\rm adv}$ (cooling flows in galaxy clusters)

ADAF around a black hole may simply advect viscously heated fluid into the black hole. A low radiative efficiency allows a high accretion rate for a given luminosity. For example, Sagittarius A$^*$ (in the galactic center) has a mass of $M_{\rm BH} \sim 4 \times 10^6\ M_\odot$ but a luminosity of only $L \sim 10^{-5} L_{\rm Edd}$. ADAF allows $\dot{M} \sim 10^{-5}\ M_\odot\ {\rm yr}^{-1}$. This is often a better fit to a spectrum than a simple SS disk.

Here are several features of an advectively dominated accretion flow for $\dot{M} < \dot{M}_{\rm crit}$

- Low accretion rates
- Optically thick, different spectra than the blackbody disk
- two temperature plasma. Ions hotter than the electrons, though the two are electrically coupled
- Steep luminosity function ($L \propto \dot{M}^2$ instead of $L \propto M$ for SS)

# 7 Active Galactic Nuclei

Active Galactic Nuclei (AGNs) are extremely luminous extragalactic sources powered by supermassive black holes in galactic centers. Observationally, we see the following characteristics

1. One highly non-thermal spectrum radiation from radio all the way to TeV energies.
2. Jets which expel energy in two opposite directions

3. Highly compact ($\lesssim 3$ pc), which indicates luminous centers
4. Strong emission lines
5. Strong UV emission (including Lyman $\alpha$ lines)
6. Jets may produce bright radio lobes when material collides with slower moving IGM (e.g. Cygnus A)
7. Rapid variability ($\sim$ minutes and longer timescales) on all frequencies
8. Broad emission from a central source (broad lines, that is).

There is a lot of different types of AGN, giving rise to a strange taxonomy which we now discuss

## 7.1 Taxonomy

Due to historical silliness, AGNs have a complex and largely disconnected set of names. These include quasars, radio galaxies, seyfert galaxies, blazars, and others. We'll go through each of these

### 7.1.1 Quasars

Originally called "radio stars", these are bright radio sources at cosmic distances that appears to be as small as a star. The nature of these objects was puzzling for a long time. We now understand them to be luminous galaxie swith compact centers. Luminosities lie in the range of $L \sim 10^{45} - 10^{49}$ erg s$^{-1}$. Around 10 percent of quasars have strong radio emission; these are called "radio loud".

### 7.1.2 Radio Galaxies

Radio galaxies look like typical elliptical galaxies but have $L_{\text{radio}} \geq 3 \times 10^{41}$ erg s$^{-1}$. A typical galaxy only has $L_{\text{radio}} \sim 10^{39}$ erg s$^{-1}$, which comes nearly entirely from supernova remnants. In radio galaxies, the large source of radio emission comes from giant radio lobes.

Faneroff & Riley further categorized radio galaxies into subtypes. Type I (FRI) are radio galaxies that are bright close to the center of the galaxy with $L_{15\ \text{GHz}} \lesssim 10^{32}$ erg s$^{-1}$ Hz$^{-1}$. Type II (FRII) have powerful jets with hot spots that have $L_{14\ \text{GHz}} \geq 10^{32}$ erg s$^{-1}$ Hz$^{-1}$. The difference between these two types are thought to be the supersonic jets found in FRII's.

### 7.1.3 Seyfert Galaxies

Seyfert galaxies are spiral galaxies with very bright, unresolved cores. We see strong emission lines from highly ionized states, like CIII, CIV, MgII, H$\gamma$, and Lyman $\alpha$. Luminosities lie in the range of $L \sim 10^{43} - 10^{45}$ erg s$^{-1}$, and these galaxies are typically radio quiet. There are subclasses for these objects as well. Sey I galaxies have broad permitted hydrogen lines, whereas Sey II galaxies only exhibit weak ones. Additionally, Seyfert galaxies are more likely than your average galaxy to be undergoing a merger.

### 7.1.4 Blazars

Blazars have polarized nonthermal emission (synchrotron and friends). They have large X-ray and $\gamma$-ray fluxes. These, too, can be classified as radio-loud and radio-quiet. We define the radio loudness via

$$R_L \equiv \log\left(\frac{F_{5\text{ GHz}}}{F_{\nu,\text{bolometric}}}\right) \tag{7.1}$$

where $F_\nu$ is the energy flux density per unit frequency. For $R_L > 1$, a blazar is radio loud (about 10-15% of blazars), and for $R_L < 1$, we say the blazar is radio quiet (85-90%).

### 7.1.5 Optical Classification

We also classify AGNs via their optical emission. Type I AGNs have a strong continuum with broad and narrow emission lines. Type II AGNs exhibit a weak continuum and only weak narrow lines.

## 7.2 The Unified Model of AGNs

After these initial observations, we have developed a unified model that asserts that each of these different objects is more or less the same, but we are viewing them at varying angles. If we look straight down a jet, we see a blazar. A little off of the jet, and we see a quasar. At even more oblique angles, we see radio galaxies. For radio quiet objects, the same picture applies, with radio quiet quasars observed at small angles, and Seyfert galaxies at larger angles. There is an obscuring torus that hides the interior of the AGN at large inclination angles.

## 7.3 Feeding the Monster

*Monday, May 20, 2013*

Different sources can feed the central black hole in an AGN. We'll briefly discuss two of them here

(a) **Stars**: Orbits on the black hole path are quickly removed from the "loss cone". These stars would be replenished by the star-star interactions in clusters around the black hole. This probably only accounts for $10^{-5}$ to $10{-}6\ M_\odot$/yr, though, so stars are essentially a negligible component in the black hole's feeding regimen.

(b) **Gas**: Accretion may be triggered by the inflow associated with galactic mergers, as AGNS seem to be correlated with mergers.

How do we estimate the mass of the central black hole is an AGN? We have observed that the black hole mass is correlated with the $B$-band intensity and the velocity dispersion in the bulge. A rough scaling relation is

$$M_{\text{BH}} = 8 \times 10^7\ M_\odot \left(\frac{L_{\text{B,bulge}}}{10^{10} L_?}\right)^{1.03} \tag{7.2}$$

where

$$L_? = 5.2 \times 10^{32}\ \text{erg s}^{-1} \tag{7.3}$$

In terms of the velocity distribution, we get

$$M_{\text{BH}} = 1.66 \times 10^8\ M_\odot \left(\frac{\sigma}{200\ \text{km s}^{-1}}\right)^{4.86} \tag{7.4}$$

We can also characterize the accretion disk at about $100-1000\,R_{\rm Sch}$ for accretion rates in the range of $\dot{M}\sim 0.01-1\ \dot{M}_{\rm Edd}$. The temperature profile behaves like

$$T(r)=6.3\times10^5\ {\rm K}\ \left(\frac{\dot{M}}{\dot{M}_{\rm Edd}}\right)^{1/4}\left(\frac{M_{\rm BH}}{10^8\ M_\odot}\right)^{-1/4}\left(\frac{r}{R_{\rm Sch}}\right)^{-3/4} \tag{7.5}$$

$T\propto\dot{M}^{1/4}$ because the radiative energy transport is proportional to $T^4$ and the dissipated energy is proportional to $\dot{M}$. So this is related to the big blue bump in the UV, so higher energy radiation must be nonthermal. We believe this to be due to upscattering of UV photons in shocks.

We have observed MeV photons, implying that pair-production occurs near the black hole with energies $\sim 2m_ec^2$, and we see radiation from different components of the AGN.

## 7.4 Broad Line Region

We see strong emission from decay after photoionization. Line widths are due to the bulk motions of material, which in AGNs can approach $10^4\ {\rm km\,s^{-1}}$, or $v/c\sim 1/30$. Such material must be within $\sim 500\,R_{\rm Sch}\leq$ pc. In clouds, radiative decay produces a line, or they can be collisionally de-excited. At an electron number density of $n_e\approx 10^9-10^{10}\ {\rm cm^{-3}}$, the volume filling factor is only $10^{-6}-10^{-5}$ and a total mass of a few $M_\odot$. Typically the cloud sizes are of the order of $10^{11}$ cm. For instance the Seyfert 1 galaxy NGS 5548 has a 50 day line delay for H$\beta$ to respond to changes in the ???

## 7.5 Narrow Line Region

We also observe line widths of $200-2000\,{\rm km\,s^{-1}}$ in forbidden lines. As a reminder, forbidden lines are transitions that are disfavored by standard quantum mechanical arguments, so their decay times are very long. Thus, they can only occur in very underdense regions. In these emitting regions, we have a number density of $n\sim 10^2-10^4\,{\rm cm^{-3}}$. So these are not collisionally de-excited. The narrow line region is spatially resolved in some Seyferts and extends about $50\,{\rm kpc}-200\,{\rm kpc}$. The volume filling factor is around $10^{-6}$ with a total mass of $M_{\rm tot}\sim 10^6\,M_\odot$ and temperatures in the range of $T\sim 10,000-25,000\,{\rm K}$, which arises from [SOMETHING] perpendicular to the disk.

## 7.6 Molecular Torus

We observe an IR bump in the QSO spectra where absorption and re-emission radiate from a central source. This dusty region has a temperature in the range of $20-80\,{\rm K}$ at 50- 150 $\mu$m. The luminosity coming from this torus is then approximately given by

$$L_{\rm IR}=2\pi R_{\rm dust}^2\sigma T_{\rm dust}^4 \tag{7.6}$$

so we can back out a radius from a temperature measurement via

$$R_{\rm dust}\sim 0.4\,{\rm pc}\left(\frac{L_{\rm IR}}{10^{46}\,{\rm erg\,s^{-1}}}\right)^{1/2}\left(\frac{T_{\rm dust}}{20\,{\rm K}}\right)^{-2} \tag{7.7}$$

## 7.7 Jets

The jets we observe from AGNs are collimated outflows from the central accretion disk. They are very radio bright and move at $v \sim c$ with Lorentz factor son the order of $\gamma = (1 - v^2/c^2)^{1/2} \sim 30$. Due to the geometry of a jet pointing near us, these can cause the motion of jet blobs to appear superluminal. Using the standard notation of $\beta \equiv v/c$, we can talk about the effect of Doppler beaming. $I_\nu/\nu^3$ is a Lorentz invariant (this will be useful). The [relativistic] Doppler formula give us an observed frequency of light via

$$\nu_{\text{obs}} = \underbrace{\frac{\sqrt{1-\beta^2}}{1+\beta\cos\theta}}_{D} \tag{7.8}$$

Then the observed spectral intensity is

$$I_\nu^{\text{obs}}(D\nu) = D^3 I_\nu^{\text{em}}(\nu) \tag{7.9}$$

For jets with $\gamma \approx 4$, ($\beta \approx 0.97$), then $D^3 \sim 1000$. Thus jets coming *at* us are beamed by a factor of 1000, where as those moving away from us are diminished by the same factor.

The radiation from jets is primarily synchrotron which usually follows a power law of the form

$$I_\nu^{\text{em}} \propto \nu^{-\alpha} \tag{7.10}$$

So the intensity at some frequency transforms via

$$I_\nu^{\text{obs}} = D^{3+\alpha} I_\nu^{\text{em}} \tag{7.11}$$

So the power law structure is preserved with the same slope but different intensity.

The jets are often well-collimated, which begs the question of how they get that way. A classic model is the "Twin Exhaust Model" put forth by Blandford and Rees (1974). Here the outflow corms constant mass injection rate into an outer medium at some pressure $P$ that decreases with the disk radius. A problem with this model is that the pressure at the source needs to be huge.

The "Pinch Effect" is another explanation invoking magnetic fields. If there is a current along the jet axis, it predicts a toroidal magnetic field that continues the jet. A big problem is that jets would probably suffer a kink, causing a Kelvin-Helmholtz instability (the model is fine for a perfectly straight jet with perfect symmetry).

In simulations using relativistic magnetohydrodynamics, a shocked jet ???? that flows back and helps to collimate the jets.

[MISSING SOME MORE BAD EXPLANATIONS: HYDRODYNAMIC]

A hydromagnetic model put forty by Blandford and Payne evokes magnetic fields that are anchored to the disk which spiral around the $z$-axis, confining the plasma along the field lines.

## 7.8 Radiation from Jets and Lobes

For example, in Cyg A, the luminosity from the radio lobes is $L \sim 10^{11} L_\odot$ and the electron density is $n_e \sim 10^{-4} - 10^{-3}\,\mathrm{cm}^{-3}$ in the lobe. This is a low enough density that the system doesn't reach a Maxwell-Boltzmann distribution. There is a magnetic field present with $B \sim 10 - 100\,\mu\mathrm{G}$. The resulting radiation is a power law with index of $\alpha \sim 0.6$. If the radiation is synchrotron, the number density as a function of energy is

$$n(E) \propto E^{-P} \tag{7.12}$$

where $P = 2\alpha + 1 \approx 2.2$ The relativistic electron spectrum comes from synchrotron emission. The electrons are accelerated in hot spots and then lose energy as they diffuse away. Meanwhile, the magnetic field is chaotic in these hot spots. The electrons have power due to synchrotron losses of

$$\left(\frac{dE}{dt}\right)_{\mathrm{sync}} = \frac{4}{3}\sigma_{\mathrm{T}} c \left(\frac{E}{M_e c^2}\right)^2 \left(\frac{B^2}{8\pi}\right) = 1.1 \times 10^{-15}\,\mathrm{erg\,s^{-1}}\ \gamma^2 \left(\frac{B}{G}\right)^2 \tag{7.13}$$

with a loss time of

$$\tau = \frac{E}{dE/dt} = \frac{6\pi m_e^2 c^3}{\sigma_{\mathrm{T}}} B^{-2} E^{-1} = 635\,\mathrm{s}\ \left(\frac{B}{1\ \mathrm{G}}\right)^{-2} \left(\frac{E}{1\,\mathrm{erg}}\right)^{-1} \tag{7.14}$$

Using the characteristic frequency for synchrotron radiation,

$$\nu_e = \frac{\omega_e}{2\pi} = \frac{eB}{2\pi m_p c} \left(\frac{E}{m_e c^2}\right)^2 \tag{7.15}$$

So the synchrotron timescale is

$$\tau_{\mathrm{sync}} = \frac{6(\pi m_e c e)^{1/2}}{2^{1/2}\sigma_{\mathrm{T}}} B^{-3/2} \nu_e^{-1/2} \tag{7.16}$$

The total energy in the lobes will come from

$$U_e \approx L_{\mathrm{sync}} \tau_{\mathrm{sync}} \tag{7.17}$$

The energy in the magnetic field is

$$U_{\mathrm{mag}} \sim \frac{VB^2}{8\pi} \tag{7.18}$$

when $V$ is the volume of the source. So the total energy is

$$U_{\mathrm{mag}} = 1.8 \times 10^{63(!)} \left(\frac{V}{\mathrm{kpc}}^3\right) \left(\frac{B}{\mathrm{G}}\right)^2 \mathrm{erg} \tag{7.19}$$

This energy is split equally between the particles and the magnetic fields.

Finally, X rays are produced in jets through synchrotron self-comptonization. Photons with a frequency $\nu$ are upscattered to frequencies $\nu' \propto \gamma^2 \nu$ after scattering off of an electron with lorentz factor $\gamma$ (with typical values of $\gamma \sim 10^4$).